SUBMITTED VERSION

Robert J. Casson, Glyn Chidlow, Jonathan G. Crowston, Pete A. Williams, John P. M. Wood
Retinal energy metabolism in health and glaucoma

Published at: http://dx.doi.org/10.1016/j.preteyeres.2020.100881

http://hdl.handle.net/2440/130370

1   ENERGY, ENTROPY, & LIFE

Energy can be defined as the capacity to do work. It can be transferred or transformed, but neither created nor destroyed: a property that emerges from the fundamental principle that the laws of physics are immutable. Energy is a bedrock requirement for all life, and almost all life on Earth ultimately derives energy from the Sun. Plants and other photosynthesizing life forms convert sunlight into chemical energy. This energy is utilized in turn by other creatures in the food chain to drive a myriad of catabolic and anabolic processes within cells and to synthesize genetic material as the substrate for Darwinian evolution.

In addition to its role as the primary energy source for the biosphere, the Sun is also a source of low entropy, a property critical for the existence of life. Entropy is conceptualized as both the loss of energy available to do work and the dispersal of energy across microstates in a system. The inviolable second law of thermodynamics states that the total entropy of an isolated system can never decrease over time. The existence of complex life, and indeed any form of life on Earth, seems to contradict the second law. As Erwin Schrödinger put it in his classic text, *What is Life?*, *"living matter evades the decay to equilibrium"*. (Schrodinger, 1944) However, Schrödinger knew that nothing ever evades the second law of thermodynamics, life's strategy is essentially to exploit the fact that the biosphere is not a closed system. Life maintains order by increasing entropy in the surrounding environment and utilizes the available energy (Gibbs free energy; G) to drive chemical reactions within cells, a phenomenon collectively known as metabolism.

2   GENERAL ENERGY METABOLISM

2.1   ATP is the energy "currency" of all cells

Metabolism refers to the total set of chemical processes that support a living organism. In some definitions, it is a *sine qua non* for life (Benner, 2010) and a foundation for abiogenesis in Haldane's primordial "*hot dilute soup*". (Haldane, 1929. ; Lazcano and Miller, 1999; Tirard, 2017) The three main purposes of metabolism are; (1) to transfer an energy source into useful cellular energy, (2) to convert food into essential molecular building blocks, such as proteins, and, (3) to eliminate cellular waste. This review is principally concerned with the first purpose, which is collectively known as "energy metabolism" or synonymously referred to as "bioenergetics".

Energy metabolism refers to the processes by which life transfers energy from a source to do cellular work. All life on Earth converts its source energy into adenosine triphosphate (ATP). There is recent evidence that the last universal common ancestor resembled modern day methanogens and probably used ion concentration gradients to generate ATP via chemiosmosis. (Weiss et al., 2016) Evolution has apparently never discovered a better alternative. Traditionally, this energy was conceptualized as being stored in the high energy phosphate bonds.(Lippman, 1941) Although convenient, this concept is misleading because the Gibbs free energy change (ΔG) is derived from the hydrolysis of ATP with water to produce ADP and inorganic phosphate. It is the chemical reaction that produces the ΔG, not energy stored in a bond. The actual ΔG produced will depend on the conditions of the reaction, including the relative concentrations of the reactants, temperature, and pressure. If the system were permitted to reach equilibrium, then ATP bonds would still be broken but the ΔG would equal zero and no useful energy would be released. ATP is formed by two interrelated processes: glycolysis in the cytoplasm and oxidative phosphorylation (OXPHOS) in the mitochondria and these are expanded on further here. (Berg et al., 2012)

2.2   Overview of Glycolysis

Glycolysis is an anaerobic process comprising 10 steps which break the 6-carbon glucose molecule into two 3-carbon pyruvate molecules (Fig. 1). In the "preparatory" phase, 2 ATP molecules are consumed; however, in the "pay off" phase 2 NADH molecules and 4 ATP molecules are produced, leading to a net gain of 2 NADH molecules and 2 ATP molecules. The pyruvate from glycolysis is then available for the citric acid cycle (CAC).
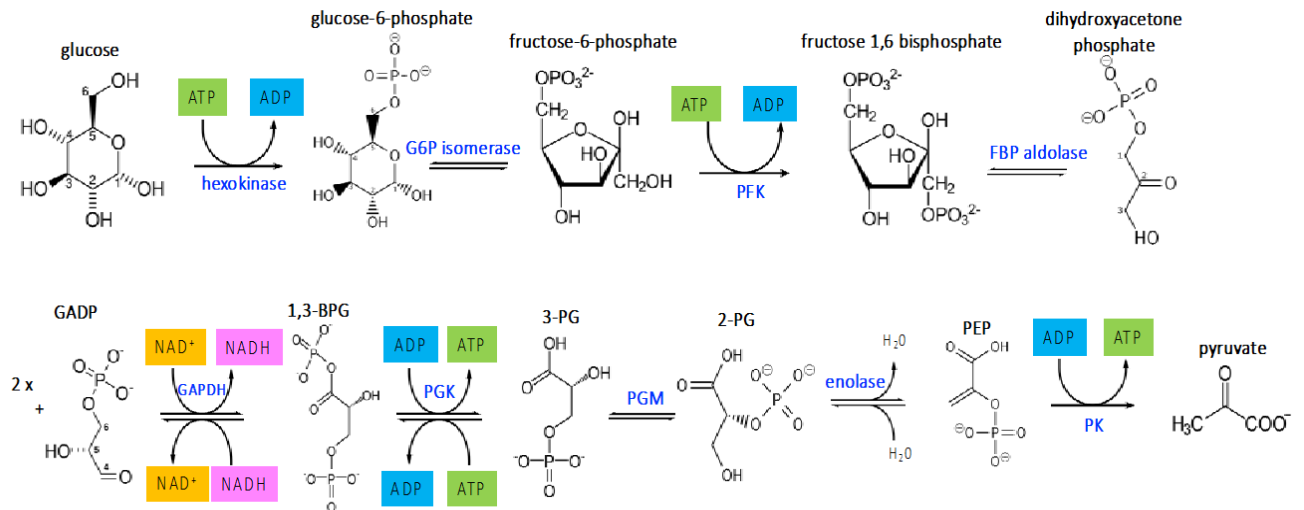

Figure 1: Glycolysis overview. Glycolysis commences with the phosphorylation of glucose by hexokinase, producing glucose-6-phosphate and consuming 1 ATP molecule. The addition of the phosphoryl group stabilizes glucose and the negative charge prevents diffusion back through the cell membrane. In addition, the cytoplasmic glucose concentration is kept low, promoting facilitated entry of glucose into the cell through the plasma membrane transporters. The next step in glycolysis is the isomerization of the aldose glucose 6-phosphate (G6P) to the ketose fructose 6-phosphate (F6P), catalyzed by G6P isomerase. This is a reversible step but usually driven towards (F6P) production because of the relatively low concentration of the product. In an irreversible reaction, another ATP molecule is consumed to phosphorylate F6P and produce fructose 1,6 bisphosphate (F1,6BP). This reaction is catalyzed by phosphofructokinase-1 (PFK), a key allosteric enzyme and the most important control site of mammalian glycolysis. This step is a commitment for the glucose molecule to proceed through glycolysis. Before this step, glucose-6-phosphate can potentially enter the pentose phosphate pathway or be converted to glucose-1-phosphate for glycogenesis. Allosteric inhibition of PFK by ATP is reversed by AMP; hence, PFK activity increases when the cellular ATP/AMP ratio is lowered, stimulating glycolysis. This second phosphorylation also produces two charged groups such that when F1,6BP is split by aldolase diffusion of substrates out of the cell is prevented. The split by aldolase produces two triose sugars: dihydroxyacetone phosphate (DHAP) and glyceraldehyde 3-phosphate (GADP). DHAP is rapidly isomerized to GADP in a reversible reaction. The next phase of glycolysis is the "pay off": two steps produce an ATP molecule from ADP. But since the 6-carbon glucose has been split into two 3-carbon molecules, 4 ATP are produced for a net gain of 2 ATP. In the first step of this pay off phase glyceraldehyde-3-phosphate oxidizes GAPDH to produce 1,3 bisphosphoglycerate (1,3BPG) and nicotinamide adenine dinucleotide (NAD+) is reduced to NADH. Electrons from the 2 NADH molecules eventually become available for the electron transport chain (ETC) in the inner mitochondrial membrane; however, the mitochondrial membrane is impermeable to NADH and the electrons are shuttled across via

the malate-aspartate shuttle and the glycerol phosphate shuttle. In the next step of glycolysis, the first ATP molecule is produced: 1,3BPG is converted to 3-phosphoglycerate (3-PG) by phosphoglycerate kinase, requiring 1 ADP molecule. 3-PG is then converted to 2-phosphoglycerate (2-PG) which is then converted by enolase into phosphoenolpyruvate (PEP). A final phosphorylation by pyruvate kinase then converts PEP to pyruvate.

2.3   Overview of the Citric Acid Cycle (CAC)

The CAC (also known as the tricarboxylic acid cycle or the Krebs cycle) is an ancient, phylogenetically conserved convergent point of metabolic pathways and an engine that extremely efficiently harvests high-energy electrons for the electron transport chain (ETC). The CAC links the production of pyruvate from glycolysis to mitochondrial respiration via the mitochondrial pyruvate carrier (MPC) and irreversible conversion to acetyl CoA, a key substrate for the CAC and endogenous lipid synthesis. The conversion of pyruvate to acetyl CoA is under complex allosteric regulation catalyzed by pyruvate dehydrogenase (PDH).

Although the traditional view holds that pyruvate is the final product of glycolysis and that this product enters the mitochondrion for oxidation via the CAC, this is not universally accepted. Recent evidence in mice indicates that the circulating level of lactate is generally much higher than that of pyruvate and that the former is a major energy substrate for all tissues except the brain (the retina was not assessed). (Hui et al., 2017) In addition, there is some evidence that lactate rather than pyruvate is directly translocated into mitochondria to fuel the CAC (the lactate shuttle theory) (Brooks, 2018). This concept is also manifest in the so-called astrocyte neuron lactate shuttle hypothesis (ANLSH). It is also important to note that the CAC is not necessarily cyclical. There are multiple entry points for substrates and many of the reactions are reversible (Fig. 2). In an excellent review, Chinopoulos emphasizes the multi-directionality of the CAC and the key stewardship role that α-ketoglutarate (αKG) plays, particularly under conditions of energy impairment. (Chinopoulos, 2013)
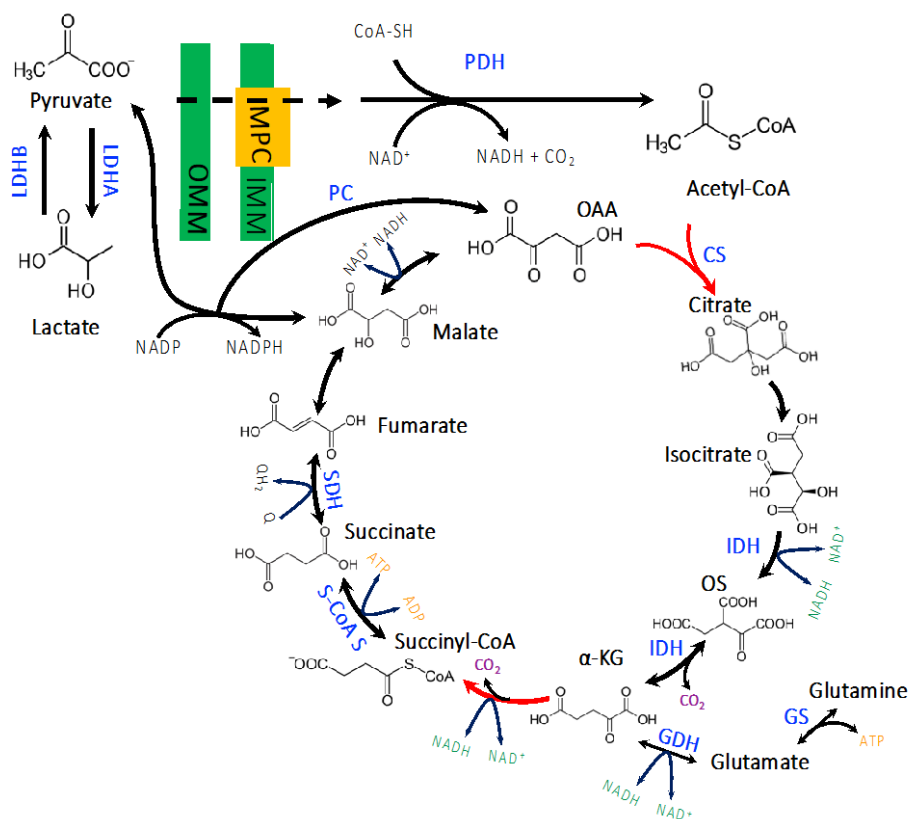

3

Figure 2: Citric acid cycle overview. For pyruvate from glycolysis to enter the CAC, it passes through the permeable outer mitochondrial membrane (OMM) and is transported through the inner mitochondrial membrane (IMM) by mitochondrial pyruvate carrier (MPC). The conversion of pyruvate to acetyl CoA occurs in the mitochondrial matrix and is a three-step process, involving the oxidation of NAD^+ to NADH. The allosteric enzyme citrate synthase then catalyzes the condensation of the 2-carbon CoA with a 4-carbon oxaloacetate molecule to form a 6-carbon citrate molecule. This step is highly exergonic (and irreversible) and is negatively regulated by ATP. In the next step, citrate is dehydrated then rehydrated with the net effect of shifting a hydroxyl group and producing isocitrate. The next two steps are catalyzed by isocitrate dehydrogenase. Oxidation of isocitrate forms oxalosuccinate whilst a molecule of NAD is reduced to NADH; oxalosuccinate is then decarboxylated to αKG and CO_2. αKG is further oxidatively decarboxylated by αKG dehydrogenase to succinyl-CoA and CO_2, whilst yielding another NADH molecule. αKG can also be formed from glutamate via glutamate dehydrogenase (GDH), and the glutamate can be formed in a reversible reaction from glutamine by glutamine synthetase (GS). Succinyl CoA synthetase converts succinyl-CoA to succinate, generating a molecule of ATP/GTP. Succinate dehydrogenase (SDH; Complex II) catalyzes the oxidation of succinate to fumarate and reduction of ubiquinone (Q) to ubiquinol (QH_2) and has a further role in OXPHOS (*vide infra*). Fumarase adds water to a double bond of fumarate yielding malate. Malate dehydrogenase oxidatively regenerates oxaloacetate and reduces another NAD molecule to NADH, completing the cycle. Two acetyl-CoA molecules are produced from each glucose molecule; hence, two cycles are required per glucose molecule. Therefore, at the end of two cycles, the products are: two GTP, six NADH, two QH_2, and four CO_2. Amino acids can also provide energy substrates for the CAC. Amino acids enter the cycle after being converted to either acetyl-CoA, pyruvate, oxaloacetate, or succinyl-CoA. Regulation of the CAC occurs at several levels. NADH and succinyl CoA negatively feedback on the key allosteric enzymes, alpha-ketoglutarate dehydrogenase and citrate synthase.

2.4   Oxidative phosphorylation

About 3 billion years ago, photosynthesizing cynanobacteria began producing oxygen as a waste product. This reacted with the iron dissolved in the Earth's ancient oceans, effectively capturing oxygen and preventing its accumulation. When the available iron substrate ran out, the atmosphere began oxygenating. (Holland, 2006) This process, known as the Great Oxygenation Event, created an environment where aerobic metabolism evolved and flourished. Although the details remain unclear, it is likely that an ancient aerobic protozoan developed a symbiotic relationship with a proto-eukaryote of probable archaeal lineage; (Williams et al., 2013) this endosymbiont evolved into mitochondria that support aerobic metabolism in almost all modern eukaryotes. (Sagan, 1967)

OXPHOS produces ~32 ATP molecules per molecule of glucose consumed; hence, the energy extracted is considerably greater than the 2 ATP produced by anaerobic glycolysis. During OXPHOS, electrons are transferred between a series of donors and acceptors within complexes located in the inner mitochondrial membrane (Fig. 3). The final electron acceptor in this ETC is O_2. The energy released by the flow of electrons is used to drive protons into the inner membrane space. The accumulated protons then have an electrochemical gradient to re-enter the mitochondrial matrix through ATP synthase, a molecular machine that catalyses the conversion of ADP to ATP. (Junge and Nelson, 2015)
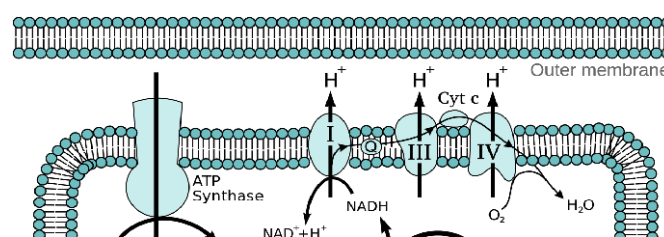
Figure 3: Oxidative phosphorylation (OXPHOS) overview. Complex 1 (NADH:ubiquinone oxidoreductase), catalyzes the transfer of electrons from NADH to coenzyme Q10 (CoQ_{10}) and translocates 4 protons across the inner mitochondrial membrane. Complex II (succinate:ubiquinone oxioreductase [SQR]; Succinate Dehydrogenase [SDH]) catalyzes the oxidation of succinate to fumarate with the reduction of ubiquinone (Q) to ubiquinol (QH_2). SDH is a complex enzyme comprising 4 subunits (SdhA-D) in the inner mitochondrial membrane. Subunit A (SdhA) is a flavoprotein with a covalently attached flavin adenine dinucleotide factor (FAD) and subunit B (SdhB) is an iron-sulfur protein. Together, they form a hydrophilic head where enzymatic activity occurs. SDH is the only enzyme that participates in both the CAC and the ETC. As a component of the ETC, it transfers electrons from succinate to ubiquinone (UbQ), referred to as the SQR activity. The SDHA subunit contains the prosthetic group FAD and converts succinate to fumarate (the SDH activity of Complex II involved in the CAC), resulting in the generation of the intermediate $FADH_2$; however, QH_2 is the final electron acceptor. Complex III (coenzyme Q: cytochrome *c* – oxidoreductase;) oxidizes the ubiquinol (QH_2). It passes the electrons onto cytochrome *c* (cyt c) and cytochrome *c* oxidase for final reduction of O_2 to water. Complex IV comprises the cytochrome proteins c, a, and a_3. This complex contains two heme groups (one in each of the cytochromes a and a_3) and three copper ions (a pair of Cu_A and one Cu_B in cytochrome a_3). The cytochromes bind an O_2 molecule between the iron and copper ions until the O_2 is reduced by the addition of two hydrogen ions to produce H_2O. Chemiosmosis is the movement of ions across a selectively permeable membrane, down their electrochemical gradient. The flow of electrons in the ETC provides energy which is used to pump hydrogen ions across the inner mitochondrial membrane. Protons then flow back across the membrane and down the potential energy gradient through ATP synthase, generating ATP in a battery-like manner by chemiosmosis. (Mitchell, 1966) (Image in the public domain from https://commons.wikimedia.org/wiki/File:Mitochondrial_electron_transport_chain—Etc4.svg)

2.5   Retinal Blood Supply

The mammalian central nervous system has evolved a highly specialized vasculature to meet the large energy demands of a metabolically active tissue and to protect sensitive neuronal information processing from blood-borne contaminants. In addition, we speculate that the fact blood is a poor transmitter of light, apropos the optical function of the eye, has produced further evolutionary adaptations in the retina. Evolutionary pressure to limit the inner retinal vascular density results in a metabolically precarious situation, rendering the retina and optic nerve particularly vulnerable to any impairment of nutrition and oxygen supply and susceptible to vascular disease.

The arterial supply to the eye is derived from branches of the ophthalmic artery, a branch of the internal carotid artery in most mammals. The photoreceptors, including their cell bodies in the outer nuclear layer, the predominance of the outer plexiform layer (OPL), and the majority of the optic nerve head (ONH) are supplied by the posterior ciliary arteries (PCAs) via the choriocapillaris. This anastomotic vascular layer corresponds to the pia-arachnoid vessels and exemplifies Dowling's conceptualization of the retina as an *"approachable part of the brain"*. (Dowling, 1987) There are watershed zones within the distribution of the PCAs that render the optic nerve head (ONH) vulnerable to impaired blood flow (*vide infra*). The inner retinal layers are nourished by branches of the central retinal artery (CRA). The dual blood supply has distinctive morphological and functional differences at the level of the capillary endothelium: the CRA-derived capillaries have tight junctions like the brain (*vide infra*) whilst the choriocapillaris has a fenestrated and polarized endothelium. (Bernstein and Hollenberg, 1965) In addition, the dual retinal blood supply is traditionally reported to produce a watershed zone at the level of the OPL (Yanoff et al., 2009); however, recent evidence indicates at least some potential for overlap. (Yu et al., 2017) The CRA bifurcates at the optic disc and the retinal arteries divide dichotomously within the superficial aspect of the nerve fibre layer adjacent the posterior vitreous face. In humans, the entire retina is supplied except the avascular extreme periphery and a foveal avascular zone (FAZ) about 0.5 mm in diameter. Using immunohistochemical methods in perfusion-fixed post-mortem human eyes, Tan *et al.* colocalized retinal capillary networks with neuronal elements. They determined the presence of four different capillary networks in the following locations: the nerve fibre layer NFL, retinal ganglion cell (RGC) layer, at the border of the inner plexiform layer (IPL) and superficial boundary of the inner nuclear layer INL, and at the boundary of the deep INL and OPL. (Tan et al., 2012) Using confocal microscopy, they further observe that the innermost and outermost capillary networks demonstrated a laminar configuration, while IPL and deep INL networks displayed a complex three-dimensional configuration. Capillary diameter in RGC and IPL networks were significantly less than in other networks. (Tan et al., 2012)

The RGC somata are located in the GCL and derive their blood supply from the retinal arteriole circulation via the superficial retinal capillary plexus. Recent optical coherence tomography angiographic evidence indicates that the radial peripapillary plexus supplies the NFL. (Campbell et al., 2017) The radial peripapillary capillaries have a unique anatomic organization because they run in parallel with the NFL axons as opposed to the lobular configurations of the superficial and deep plexuses. This vascular plexus is dense in the peripapillary region and decreases in density with distance from disc along the maculopapillary axis. (Campbell et al., 2017) The radial peripapillary capillary plexus supplies the NFL near the ONH and has a unique anatomic organization running in parallel with the NFL axons. The foveal avascular zone in primates notwithstanding, whether the average density of capillaries in the retina differs from the density in the brain, to our knowledge, has never been determined.

There are important interspecies differences in the inner retinal vascularization: only primates have a characteristic macula and FAZ; rodents have a spoke-like arrangement of vessels centred on the optic nerve and although they lack a macula, they have a vascularized (holangiotic) retina like primates; in the rabbit, vessels are confined to a broad horizontal band within a streak of myelinated nerve fibres (merangiotic pattern); in the guinea pig the retinal blood vessels are restricted to the direct vicinity of the optic disc (paurangiotic pattern); and the avian retina is completely avascular (anangiotic pattern) (De Schaepdrijver et al., 1989).

2.6   The Blood Retinal Barrier (BRB)

The BRB has an inner and outer component (Fig. 4). The inner BRB is analogous to the blood brain barrier, a functional neurovascular structure comprising the tight junctions of endothelial cells, pericytes and

astrocyte foot processes. (Cunha-Vaz, 1979) In the BRB, the Müller glial cells substitute for the astrocytes in the deeper capillary layers. (Tout et al., 1993) Brain and retinal endothelial cells contain extremely tight cell-cell junctions that are distinct from the tight junctions of endothelia and epithelia elsewhere in the body. (Kniesel and Wolburg, 2000) Unlike other endothelial cells, which are predominately glycolytic, brain endothelial cells have many mitochondria and are more reliant on oxidative metabolism. (Oldendorf et al., 1977) Recent studies have established the critical role of mitochondria in maintaining the blood brain barrier. (Doll et al., 2015) Furthermore, in the brain, astrocytes induce and support endothelial tight junctions, and there is evidence that Müller glial cells play a similar role to support the barrier function in the retina (Tout et al., 1993) and regulate intra-retinal ion and water flow. (Reichenbach et al., 2007) The outer BRB is formed by the tight junctions between the RPE cells (analogous to ependymal cells lining the cerebral ventricles), preventing contaminants from the choroidal blood supply from reaching the subretinal space.
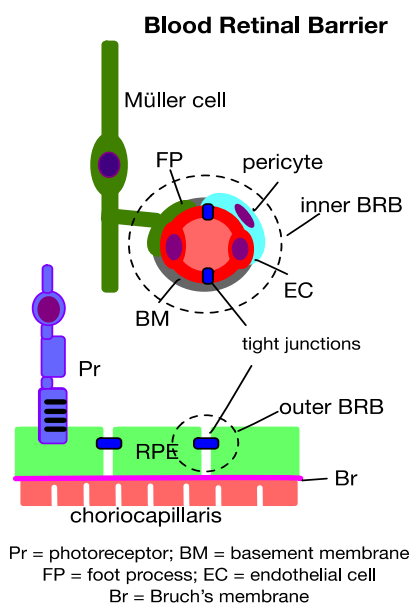

Figure 4: **The blood retinal barrier** (BRB) is composed of both an inner and outer barrier. The inner BRB consists of the tight junctions of the endothelial cells of the capillaries, pericytes and macroglial foot processes. The outer BRB consists of the tight junctions between the retinal pigment epithelial cells (RPE)

2.7   Optic nerve head blood flow

The optic nerve head (ONH) describes the portion of the optic nerve as it exits the globe and the axons pass through the lamina cribrosa. The ONH is principally supplied by branches of the posterior ciliary artery (PCA) with the most superficial nerve fibre layer supplied by branches of the central retinal artery. Anteriorly, the ONH is exposed to the intraocular pressure (IOP), and posteriorly to the cerebrospinal fluid pressure. The blood supply to the prelaminar region, which lies between the surface nerve fibre layer and the lamina cribrosa is controversial. Hayreh has reported that it is supplied by the fine centripetal branches from the peripapillary choroid; (Hayreh, 1996, 2001) however, others have reported that it is supplied by branches of the PCA. (Onda et al., 1995) The lamina cribrosa region is entirely supplied by centripetal branches from the short PCAs, either directly or from the circle of Haller and Zinn formed by the short PCAs. (Hayreh, 1996) The presence of the circle of Zinn-Haller is also controversial and appears to be a variable microvascular landmark supplying the lamina cribrosa. The retrolaminar region always has a

peripheral centripetal vascular supply from the pial plexus and may also receive centrifugal branches from the central retinal artery. (Hayreh, 1996) The venous drainage is via the central retinal vein except that the prelaminar region also drains into the peripapillary choroidal veins. (Hayreh, 1996) The vessels in the ONH lie in its septa so that the distribution of the septa corresponds to a distribution of the blood vessels. (Hayreh, 1996, 2001) Importantly, there are watershed zones between the distribution of the various PCAs. (Hayreh, 2001) Based on a consilience of evidence using various techniques, Hayreh notes *"in almost all of the patterns, the watershed zone passes through the ONH; that makes the watershed zones play a very important role in ONH ischemic disorders, because the part of the ONH that is located in the watershed zone is most vulnerable to ischemia, and the most vulnerable position is when the entire ONH lies in the centre of a watershed zone."* (Hayreh, 2001)

2.8   Retinal Oxygen Consumption and ATP demands

The brain has a large oxygen demand, reflecting the high energy cost of neuronal computation. The human brain consumes O_2 at a rate of approximately 3.5 ml/min/100 g. (Clarke and Sokoloff, 1999) Therefore, the O_2 demand for an average human brain weighing 1400g is approximately 50 ml/min. This fact is frequently emphasized in the literature by noting that total body O_2 consumption is approximately 250 ml/min; hence, the brain, although only 2% of body mass consumes 20% of the oxygen. (Clarke and Sokoloff, 1999)

However, per unit weight, the retinal oxygen demands are even greater. In 1968, Banks Anderson Jr. recorded the time to blackout in healthy volunteers breathing variable concentrations of oxygen. The subjects were required to report when an 8 x 88 mm vertical black line at 1.8 m completely disappeared. From these data, he estimated that the oxygen requirement of the retina was approximately 7 ml/min/100 ml tissue. Using mathematical modelling, Linsenmeier *et al.* have calculated rates of oxygen consumption in the outer retina of approximately 4.5 ml/min/100 ml. In a comprehensive review, Yu *et al.* (Yu et al., 2013) noted that vascularized inner retinas (like those of rats and humans) utilize both glycolytic and OXPHOS ATP production. Using elegant microelectrode O_2 tension recordings *in vivo*, Yu and Cringle *et al.* have reported important differences in the O_2 consumption rates between species and between the inner and outer retina (Fig. 5). (Cringle et al., 2002; Yu and Cringle, 2001) In a 4-layer mathematical model of the avascular guinea pig retina, the outer retina consumes O_2 at a rate of 2.07 ml/min/100 g whereas the glycolytic inner retina has a consumption rate of 0.12 ml/min/100 g. They conclude that in the avascular retina, the O_2 consumption of the photoreceptors essentially dictates the O_2 level in the inner retina. In an 8-layer model of the vascularized rat retina, they note that the dominant oxygen consuming layers are the inner segments of the photoreceptors, the OPL and the deeper aspect of the IPL.

Measurements of the oxygen consumed by isolated insect retinas indicate that in the drone bee retina each photoreceptor consumes 2×10^9 ATP molecules per second, (Tsacopoulos et al., 1994) and photoreceptors in the blowfly retina consume 7×10^9 ATP molecules per second. (Laughlin et al., 1998) Okawa *et al.* have reported that the total energy consumption of mammalian rods declines from about 10^8 ATP s^{-1} in darkness to less than a quarter of this value in bright light. (Okawa et al., 2008) This is consistent with the observation by Ames *et al.* that, in rabbits, the dark current accounted for approximately 40% of the retina's O_2 consumption. (Ames et al., 1992) We must be mindful that rates of retinal ATP and O_2 consumption reported in the literature are likely to be species dependent; in particular, in mammalian retinas, they will depend on the retinal vascularization.

RGC   Müller
Amacrine   Photoreceptor
Bipolar   RPE
Horizontal   Choroid
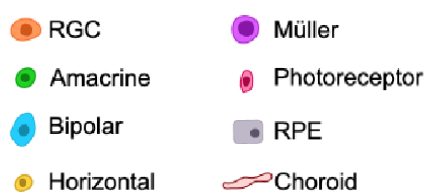
45 mmHg

IS/OS
ONL
OPL

Figure 5: Retinal oxygen consumption by retinal depth. Basic retinal structure in animals with vascularized retinas (such as rodents and humans). Black curved line represents oxygen

2.9 Retinal energy demands in context

The retina is often reported to have one of the highest energy demands of any tissue. From the discussion above, we note that the retina has a large energy demand per unit weight, but that the energy consumption per cell is not extravagant. For example, resting mammalian cortical neurons consume approximately 4.7×10^9 ATP molecules per second (Zhu et al., 2012) and fibroblasts consume approximately, 1×10^9 ATP molecules per second. (Flamholz et al., 2014) The relatively large energy demands of the retina per unit weight compared to the brain are due the high neuronal density of the retina, particularly the tightly-packed photoreceptors. The human cerebral cortex has an average weight of 1250 g and contains 25 billion neurons (slightly below expectations for a primate brain), giving a cortical neuron density of 2×10^7 cells/g. (Herculano-Houzel, 2009) This compares to the human average photoreceptor density of approximately 6×10^8 cells/g. Hence, impairment of function of retinal cells should not immediately be attributed to an intrinsically large energy demands but may occur when insufficient nutrients and oxygen are not reaching their targets.

3 RETINA ENERGY METABOLISM

Retinal energy metabolism is complex. The retina is not a structurally or functionally homogenous structure, and although aspects of general metabolism undoubtedly apply, the various retinal cell subtypes have specific tasks with varying energy demands occurring in specific microenvironments with respect to nutrient and oxygen supply. Unravelling the retinal energy metabolism at a cellular level is a challenging task. Before turning to the metabolism of the retinal cell subtypes, there are two important bioenergetic phenomena with particular relevance to the retina that are worth discussing: the Warburg effect and the Pasteur effect.

3.1 The Warburg Effect

In the 1920s, Otto Warburg and his group at the Kaiser Wilhelm Institute noted that cancerous tissue tended to make ATP via glycolysis despite the presence of abundant oxygen. This phenomenon was

described as aerobic glycolysis and later became eponymously known as the Warburg effect. It is defined and measured by the production of relatively large amounts of lactate in the presence of oxygen. Warburg's team noted that animal retinas also displayed aerobic glycolysis but attributed the finding to non-physiological *ex vivo* conditions, concluding that aerobic glycolysis was unlikely to occur in the normal retina *in vivo*. (Warburg, 1930) A prevailing explanation for the phenomenon in cancer is the notion that proliferating cells divert glycolytic metabolites towards biosynthesis rather than towards oxidative phosphorylation. (Vander Heiden et al., 2009) Metabolic reprogramming, with a shift to aerobic glycolysis is a hallmark of cancer. Evidence indicated that a specific isoform of pyruvate kinase M2 (PKM2) served as a master switch in most cancers, "directing traffic" in glycolysis between ATP production and diversion of intermediates into the pentose phosphate pathway to supply carbon atoms for amino acid synthesis. (Christofk et al., 2008) Based on these ideas from the cancer literature, we previously hypothesized that the Warburg effect in the retina may represent the biosynthetic demands of photoreceptor outer segment turnover. (Casson et al., 2013) This hypothesis was supported by the identification of PKM2 in mammalian photoreceptors. (Casson et al., 2016; Lindsay et al., 2014) We further identified that mammalian photoreceptors contain dimeric and tetrameric PKM2 as well as LDH-A. Dimeric PKM2 has a lower affinity for its natural substrate, phosphoenol pyruvate (PEP), than the predominant tetrameric form, and its presence will slow glycolytic flux and promote the accumulation of upstream substrates. This is consistent with the ability of a cell to switch between energy production and biosynthesis like a proliferating tissue, possibly due to demands of opsin synthesis. (Casson et al., 2016) However, recent evidence form the cancer literature (from early proponents of the biosynthesis hypothesis) indicates that glucose carbon contributes only about 20% of the total carbon mass of selected cancer cells (the majority of carbon atoms in anabolic pathways were from amino acids). (Hosios et al., 2016) Unpublished findings from our own laboratory also do not support the biosynthesis hypothesis as an explanation for the Warburg effect in the retina. However, it is not definitively ruled out. Furthermore, the biosynthetic hypothesis becomes logically problematic when we consider that if the carbon atoms from glucose are being used for biosynthesis, how are they also being used to make lactate? (Locasale and Cantley, 2011)

We take this opportunity to provide our current thinking on the Warburg effect in the retina. Firstly, there is convincing evidence that the photoreceptors are responsible for the Warburg effect in the retina, at least in terms of the quantity of lactate produced under physiological conditions. (Chertov et al., 2011; Graymore and Tansley, 1959; Wang et al., 1997a, b) However, this may be largely a function of their dominant contribution to retinal cell numbers. It is plausible, for example, that other retinal cell types produce and efflux more lactate per cell than the photoreceptors. This is an area of current investigation in RJC's laboratory. Furthermore, the critical "decision-making" for the Warburg phenomenon rests with pyruvate. Why is pyruvate converted to lactate when it could apparently more profitably proceed downstream? Inhibition of PDH is a straightforward explanation under hypoxic conditions (*vide infra* the Pasteur effect). But what about under normoxic conditions?

 A possible explanation for the Warburg effect in normal cells is that it is a manifestation of both high energy demands and relative reduction in O_2 supply under the paradigm that lactate rather than pyruvate is, in fact, the end point of glycolysis. (Brooks, 2018; Rogatzki et al., 2015) This framing removes the need for pyruvate to "make a decision". The concept is supported by the high lactate dehydrogenase (LDH) activity of many cell types (including photoreceptors) and hypothesizes that lactate is a critical fuel source entering the mitochondria, converting to pyruvate and generating NADH in a reaction catalysed by mitochondrial LDH; hence, serving as an indirect substrate for the CAC and OXPHOS. In this paradigm whenever glycolytic activity increases, lactate production also increases irrespective of the oxygen support. When energy demands are not matched by O_2 supply, or CAC enzymes deplete, lactate cannot be processed in downstream energy metabolism pathways and begins to accumulate; excess lactate is then effluxed via monocarboxylate transporters (MCTs) and potentially utilized by neighbouring cells within the

bioenergetic ecosystem. Importantly, the O_2 limitation does not necessarily need to be at hypoxic levels. Furthermore, it would not be inconsistent for cells displaying the Warburg effect to have plentiful mitochondria. We suggest that photoreceptor ATP demands are sufficiently high and O_2 is sufficiently limited under physiological conditions such that lactate accumulates; hence, explaining the Warburg effect in the retina. However, this remains speculation, and understanding the teleology underpinning the Warburg effect in both cancer and the retina requires further study.

3.2   Pasteur effect

The Pasteur effect refers to the increase in glycolysis when oxygen is limited, or conversely the reduction of glycolytic fermentation when oxygen is abundant. (Pasteur, 1861) The phenomenon is a cellular adaption to hypoxia and is underpinned by hypoxia inducible factors (HIFs).

HIFs are heterodimeric transcription factors that reprogram energy metabolism when oxygen is scarce. They comprise an oxygen-dependent α-subunit and a constitutively expressed β-subunit. In the presence of normal oxygen tension, the α-subunit is hydroxylated by prolyl hydroxylases (PHD) creating a binding site for von Hippel-Lindau tumor suppressor protein (pVHL) which then guides the ubiquitination and proteasome degradation of HIF subunits. If HIF is not degraded, it promotes glycolysis and lactate production through transcriptional upregulation of glucose transporters (SLC2A1 and SLC2A3), glycolytic enzymes (HK and PK), and lactate dehydrogenase A (LDHA). (Kim et al., 2006) HIF1 also suppresses pyruvate metabolism through the CAC by activating pyruvate dehydrogenase kinase 1 (PDK-1), an inhibitor of PDH. (Kim et al., 2006) Under hypoxic conditions but in the absence of HIF-1α, mammalian cells exhibit decreased levels of glycolysis and corresponding reduction in lactic acid production with markedly reduced ATP levels. (Seagroves et al., 2001) Hence, the stabilization of HIF in hypoxia and its subsequent effects on energy metabolism are essentially the mechanistic explanation for the Pasteur effect. Whether or not HIF is stabilized in the retina under physiological conditions is unclear. HIF is a notoriously difficult protein to detect by immunohistochemistry or immunoblotting. Hughes *et al.* reported that both human and rat retinas displayed prominent immunostaining of HIF-1α in nuclei of most cell types in inner and outer nuclear layers and the GCL and identified HIF in human retina by immunoblotting of nuclear extracts. (Hughes et al., 2010) This is an important finding; however, to our knowledge it has not been corroborated by other researchers. However, Williams *et al.* have shown that HIF is expressed by RGCs in the DBA/2J model of glaucoma, suggesting that there is a hypoxic element in this model and that RGCs do display a Pasteur effect. (Williams et al., 2017b) Using immunohistochemical techniques, we have shown that ocular hypertension caused selective hypoxia within the laminar ONH in a rat model of glaucoma in eyes graded as either medium or high for axonal transport disruption. Hypoxia was always present in areas featuring injured axons, and, the greater the abundance of axonal transport disruption, the greater the likelihood of a larger hypoxic region. (Chidlow et al., 2017)

Whether HIF is required for the Warburg effect in the retina is unknown. If HIF was present under physiological conditions and was required for production of relatively large amounts of lactate, then the Warburg effect in the retina would essentially be a misnomer. The mystery would be resolved by explaining the apparent Warburg effect as a manifestation of the Pasteur effect. HIF-1 is notoriously difficult to detect *in vivo,* but the presence of HIF-target gene/protein upregulation in the retina would provide some evidence in favour of a HIF-induced effect. We note that both PKM2 and LDHA are target genes for HIF-1 and both are heavily expressed in photoreceptors of vascularized retinas under physiological conditions. However, other target genes such as pyruvate dehydrogenase kinase-1 are not.(Sradhanjali et al., 2017) The situation is further complicated by the fact that other regulators such as c-Myc can activate HIF-responsive genes. Further study is required to determine the role of HIF and/or other regulators of the Warburg effect in the retina.

3.3   Astrocyte neuronal lactate shuttle hypothesis

The preferred energy substrate of cortical neurons remains highly controversial. The traditional notion that glucose was their major energy substrate was challenged in 1994 by Pellerin and Magistretti *et al.,* who provided evidence that astrocytes, not neurons, metabolize glucose, and transport lactate to the neuron, which is converted to pyruvate as a substrate for the Krebs cycle and OXPHOS. (Pellerin and Magistretti, 1994) They reported that astrocytic lactate production is calibrated by neuronal glutamate production, providing a feedback between energy supply and neurotransmission demands. This concept became known as the ANLSH. However, this concept has become highly controversial, with some researchers in favour (Bouzier-Sore et al., 2003), but others criticizing it. (Chih et al., 2001)

The existence of a glial-neuronal energetic shuttle in the retina was first proposed by Tsacopoulos *et al.* from study of the drone bee retina, which features a simple structure of only two cells types: glia and photoreceptors. Using retinal slices, they showed that photoreceptor function could be maintained for a number of hours despite glucose being uptaken exclusively by the glial cells not photoreceptors (Tsacopoulos et al., 1987). They concluded that there must be an energy substrate transfer from glia to photoreceptors. Turning their attention to the mammalian retina, the same researchers published a landmark study using the guinea pig retina, in which they revealed a net transfer of lactate from the highly glycolytic Müller cells to photoreceptors that served to fuel mitochondrial oxidative metabolism and glutamate resynthesis (Poitry-Yamate et al., 1995). Intriguingly, however, an expanding body of work conducted on rodent retinas in recent years does not support the existence of a metabolic transfer of monocarboxylate from Müller cells and photoreceptors. This is despite the fact that rodent retinas display a high rate of aerobic glycolysis. (Winkler, 1981b) It transpires that it is photoreceptors, rather than Müller cells, that produce large amounts of lactate in the presence of abundant oxygen. (Chinchore et al., 2017; Petit et al., 2018; Wang et al., 1997a; Winkler, 1981a) Accordingly, photoreceptors express a specific complement of glycolytic isoenzymes, including hexokinase II, pyruvate kinase M2, and LDH-A, that are more commonly found in glycolytic tumour cells (Fig. 6). (Casson et al., 2016; Chinchore et al., 2017; Lindsay et al., 2014; Petit et al., 2018). These findings have prompted a radical shift in thinking about energy metabolism in the different cell layers of the retina. How can these conflicting theories be reconciled? The explanation lies in the fact that there is a fundamental difference in metabolism between vascularised and avascular retinas, as depicted in Figure 7, which represents our own unpublished data. In avascular retinas, such as those of rabbit and guinea pig, Müller cells express abundant glycolytic enzymes together with the isoform of lactate dehydrogenase (LDH-A) that favours conversion of pyruvate to lactate, while photoreceptors express the isoform (LDH-B) that favours conversion of lactate to pyruvate. Such a
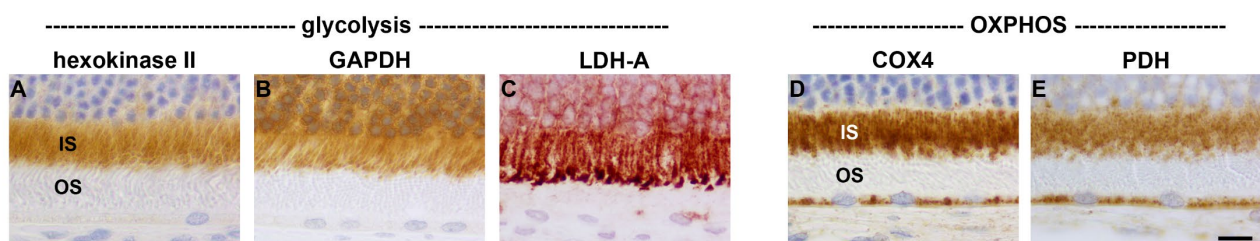
Figure 6: Expression of glycolytic and mitochondrial enzymes in photoreceptor segments. Representative immunolabelling of the aerobic glycolytic enzymes hexokinase II (A) and LDH-A (C), as well as GAPDH (B), plus the mitochondrial OXPHOS enzymes cytochrome c oxidase (COX4; D) and pyruvate dehydrogenase (PDH; E) are shown. In each case, robust labelling of inner, but not outer, segments is observed. GAPDH and LDH-A are also associated with rod somas in the outer nuclear layer. Scale bar: 12 μm. IS, inner segments; OS, outer segments.

profile is consistent with Müller cell to photoreceptor lactate transfer, as proposed by Poitry-Yamate *et al.* (Poitry-Yamate et al., 1995) In contrast, in vascular retinas, such as rat and mouse, it is photoreceptors that express abundant glycolytic enzymes together with LDH-A. Of note, negligible LDH-B is detectable in rat and mouse photoreceptors. Such a profile is consistent with glucose acting as the primary fuel source for photoreceptors and of there being no significant contribution from Müller cells, which do not display a profile compatible with aerobic glycolysis. The energetic metabolism of RGCs is considered in section 4.2.
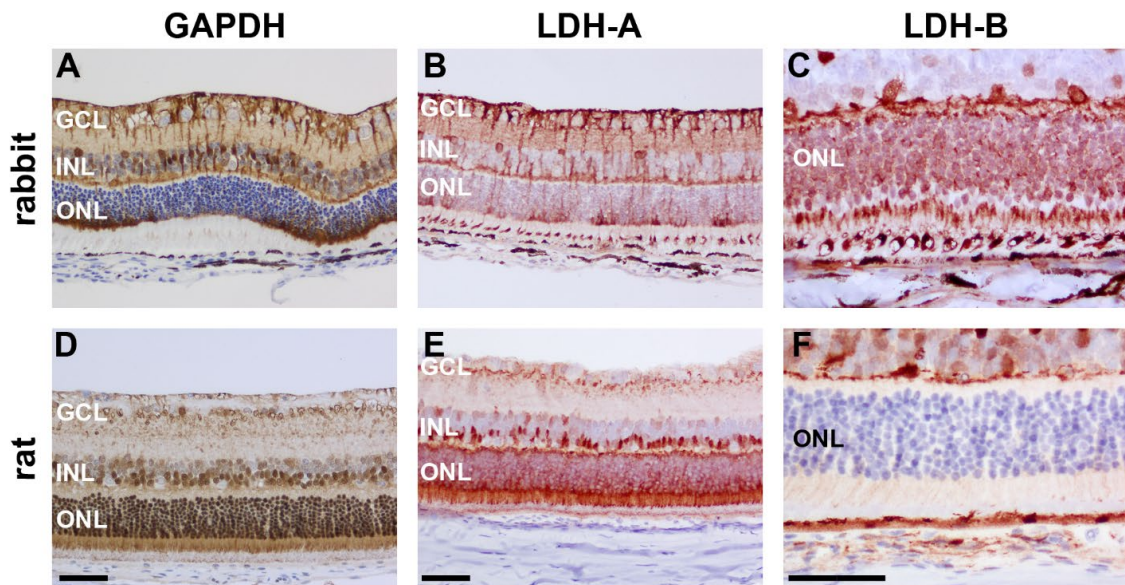
Figure 7: Expression of GAPDH, LDH-A and LDH-B in vascular and avascular retinas. Markedly different patterns of expression are observed in the avascular rabbit retina compared to the vascular rat retina. In rabbit retina, GAPDH (A) and LDH-A (B) are both chiefly, but not exclusively, associated with Müller cells, with expression of both enzymes encompassing the soma and processes that traverse across the retina. LDH-B (C), in contrast, is robustly expressed by rod and cone photoreceptors. In rat retina, GAPDH (D) and LDH-A (E) are both strongly associated with photoreceptor somas and their inner segments as well as bipolar cells, but are barely detectable in Müller cells, while LDH-B (F) is essentially absent from rod and cone photoreceptors. Scale bars: 60 μm. GCL, ganglion cell layer; INL, inner nuclear layer; ONL, outer nuclear layer.

4   RGCs

4.1   RGC anatomy and function

RGCs serve as analogue to digital converters, receiving visual information encoded in the form of graded responses and transmitting digitized information encoded as action potentials to targets in the brain. RGCs are shift-invariant linear systems meaning that their output (firing rate) is determined by a summation of the input stimuli (contrast) and is directly proportional to change in the stimuli independent of time.(Enroth-Cugell and Robson, 1966) Their somata are located in the ganglion cell layer and their dendrites arborize with amacrine and bipolar cells in the IPL. Their axons comprise the optic nerve. For optical purposes, the intraocular portion of the RGC axon in most mammals is unmyelinated. These fibres make an indirect and sometimes tortuous path through the lamina cribrosa at the optic nerve head before becoming myelinated and continuing to the lateral geniculate nucleus and other targets. There are several major classes of RGC and over 25 subtypes have been described. The parvocellular RGCs (midget ganglion cells) are the anatomical conduits of the P pathway which serves high-acuity spatial vision and red–green colour vision. The magnocellular RGCs (parasol ganglion cells) comprise the M pathway, serving contrast, motion and luminance change detection. In the P pathway, cones synapse with midget bipolar cells which in turn contact midget ganglion cells. (Calkins et al., 1994) In the M pathway, diffuse bipolar cells receive input from multiple cones and provide output to parasol cells (Boycott and Wassle, 1991) Another retino-thalamic pathway, the koniocellular (K) pathway has not been full characterized and appears to serve various functions. (Hendry and Reid, 2000) Many rods converge onto a rod bipolar cell in the OPL where divergence occurs to amacrine cells, the most important of which are the AII and the A17 cells. (Kolb, 1970; Kolb and Famiglietti, 1974) Rod bipolar cells do not synapse with RGCs directly; however, there is recent evidence from an animal model that dysfunction of this rod-bipolar-amacrine-RGC pathway early generalized loss of retinal sensitivity characteristic of glaucoma is due to dysfunction of the rod-bipolar pathway. (Pang et al., 2015)

4.2   RGC energy metabolism

The RGC is fundamentally a tripartite structure, comprising a soma, dendrites, and axon. Each component serves different functions and is located in a different milieu; hence, the nutrient delivery and energy demand is non-uniform within single cells. Others have highlighted the nature of RGCs as a compartmentalized structure (Whitmore et al., 2005; Yu et al., 2013) and we have previously emphasized the importance of this concept in the context of neuroprotection. (Casson et al., 2012a)

4.2.1   *Energy metabolism of RGC somata*

Using microelectrode oxygen tension recordings in rats, Yu and Cringle have observed that the outer region of the IPL has a low oxygen tension, which can conceivably be attributed to a high rate of oxygen consumption. (Yu and Cringle, 2001) This region (sublamina a) corresponds to the sublaminar component of the IPL which contains the synaptic connections of the OFF bipolar cells and the OFF ganglion cells. (Famiglietti and Kolb, 1976) This is consistent with the finding that sublamina a in cats and ferrets has more intense immunostaining with cytochrome c oxidase (a marker of mitochondrial density). (Famiglietti and Kolb, 1976) And is also consistent with the concept that the synapse is the most energy demanding component of the neuron. (Harris et al., 2012) Furthermore, although not entirely consistent in the literature, the OFF ganglion cells tend to be particularly vulnerable to IOP-induced injury. (Della Santina et al., 2013) Why these subtypes would require more O_2 than their ON counterparts is, however, unclear.

Yu and Cringle report a relatively low rate of oxygen consumption in the GCL and in the inner portion of the IPL of the rat retina. (Yu and Cringle, 2001) This observation extrapolates to a relatively low oxygen consumption rate of RGC somata in the vascularized mammalian retina, implying that RGCs may utilise aerobic glycolysis to help meet their energy needs, as occurs predominantly in avascular inner retinal

neurons.(Lowry et al., 1961) It is certainly the case that RGCs in the vascular retina express glycolytic enzymes, indicating that these neurons have the requisite machinery to take up and metabolise glucose directly (Fig. 7A-C). Yet, the extrapolation to a low oxidative profile is not consistent with the large amounts of mitochondrial proteins that we have observed in RGC somata in vascularized retinas. We have previously assessed the expression of eight mitochondrial proteins, including mitochondrial pyruvate carrier 1 and PDH, using immunoblotting and immunohistochemistry, and, assessed activity of cytochrome c oxidase, succinate dehydrgogenase, and isocitrate dehydrogenase using enzyme histochemistry on unfixed tissue sections of vascularized retinas. Strong, punctate labeling for all mitochondrial proteins was observed in RGC somata, together with high enzyme activity in the IPL and surrounding RGCs. The combined data indicate that RGCs are readily able to oxidise pyruvate via the CAC (Fig. 7D-F). This conclusion is further supported by analysis of LDH activity and subunit expression. LDH activity is widespread throughout the retina (Fig. 7G), but in the case of inner retinal neurons this activity must predominantly derive from LDH-B since LDH-A is only sparsely detectable (Fig. 7H). Of particular interest is the robust expression of the LDH-B isoform in some RGCs. This finding implies that RGCs have the ability to use lactate as a metabolic fuel for the CAC, whereas it would seem less likely that they habitually convert pyruvate to lactate via aerobic glycolysis in a manner akin to photoreceptors.

Can it be concluded, therefore, that RGCs utilise lactate as their primary fuel source? We would argue not. In previous work from our laboratory, we showed that cultured neurons preferentially metabolized glucose over lactate (Wood et al., 2005), while intraocular lactate delivery was not able to provide protection to the rat retina subjected to ischemia-reperfusion injury (Casson et al., 2004), and, inhibition of lactate transport did not exacerbate ischaemic retinal injury. (Melena et al., 2003). Furthermore, autoradiographic studies by Winkler *et al.* have shown glucose to be the preferred energy substrate of retinal neurons. (Winkler et al., 2003) These findings can be explained, however, if one considers that RGCs are actually programmed to be remarkably flexible in their ability to utilise different substrates for energy production. Thus, although glucose may be the preferential fuel for energy production, other substrates can be used in certain circumstances. Indeed, our recent unpublished work has demonstrated this effect clearly: in the absence of all other potential energetic substrates, retinal neurons including RGCs, remain viable in the presence of either glucose, pyruvate, or, of particular interest, lactate, (Fig. 8I-M). Clearly, then, *in situ*, RGCs can metabolise various energetic substrates when circumstances dictate.
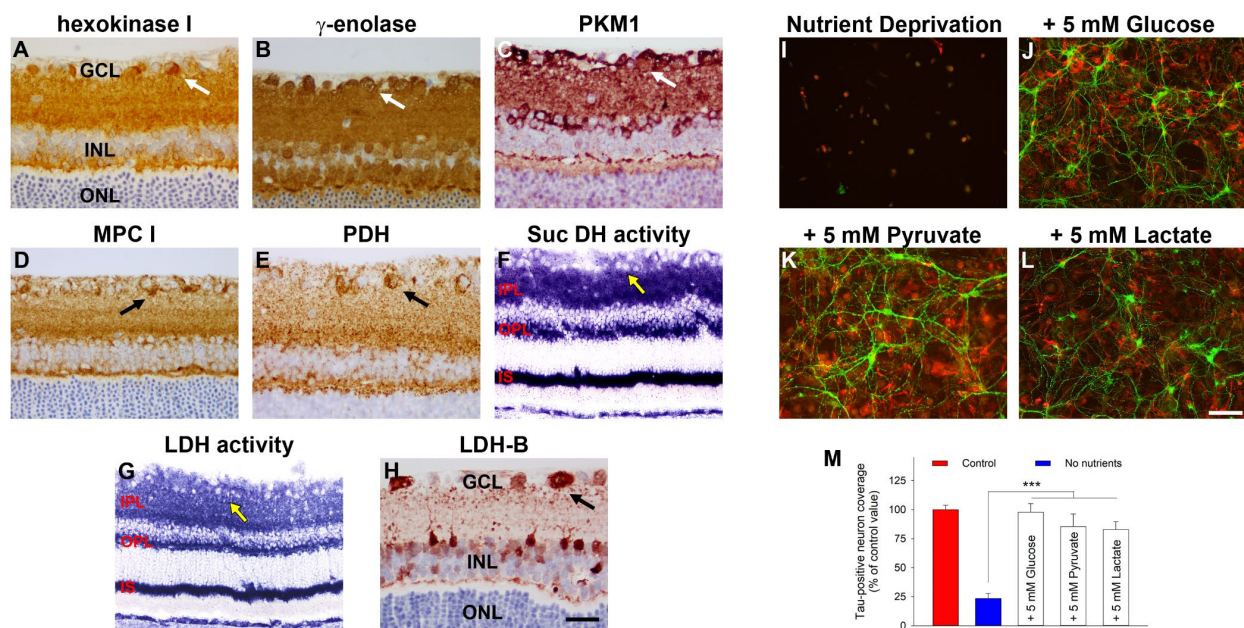
Figure 8: Energy production and utilization in the rat retina. (A-H) Expression and activity of glycolytic and mitochondrial enzymes in rat retina. (A-C) Representative images of the glycolytic enzymes hexokinase 1 (A), neuron-specific enolase (χ-enolase; B) and PKM1 (C) immunolabeling in the retina. For all three enzymes, immunolabelling is enriched in inner retinal neurons, notably RGCs (arrows), and their processes in the inner plexiform layer. (D-F) Representative images of mitochondrial pyruvate carrier 1 (MPC1; D) and pyruvate dehydrogenase (PDH; E) immunolabeling, and succinate dehydrogenase (Succ DH; F) activity, in the retina. MPC1 and PDH proteins display similar patterns of distribution with strong, punctate labelling of the inner and outer plexiform layers and RGC somas (arrows). Highest activity of Succ DH is observed in photoreceptor inner segments, with both plexiform layers also robustly labeled, including high activity surrounding RGCs (arrow). (G, H) Representative images of total LDH activity (G), and LDH-B (H) immunolabeling, and in the retina. As for Succ DH, highest LDH activity is observed in photoreceptor inner segments, with both plexiform layers also showing robust activity, including high activity surrounding RGCs (arrow). LDH-B immunolabelling is primarily observed in RGCs (arrow), amacrine cells and horizontal cells. (I-M) Energy substrate utilization by cultured rat retinal cells. Neurons including ganglion cells are labelled with antibody to tau (green) and astrocytes/Muller glial cells with antibody to vimentin. (I) Removal of all possible energy substrates from medium for 24 hours leads to catastrophic loss of all cells. Addition of 5 mM glucose (J), 5 mM pyruvate (K) or 5 mM lactate (L) during incubation period preserves both neurons and glial cells. Quantification of neuronal preservation indicates that this effect is of statistical significance (M). *** $P < 0.001$, when comparing nutrient deprived cultures with those with added glucose, pyruvate or lactate, by one-way ANOVA followed by Dunnett's test for multiple comparisons. Scale bar: A-C, D, E, H = 30 μm; F, G = 60 μm; I-L = 40 μm. GCL, ganglion cell layer; IPL, inner plexiform layer; INL, inner nuclear layer; OPL, outer plexiform layer; ONL, outer nuclear layer; IS, inner segments.

4.2.2   Energy metabolism of RGC dendrites

RGC dendrites synapse with bipolar cells and amacrine cells in the inner plexiform layer, receiving excitatory and inhibitory signals, respectively. The input signals at the level of the synapse summate and continuously modify the electrical status of the membrane. This analogue input ultimately determines the firing of the action potential at the axon hillock resulting in an "all or none" response. (Adrian, 1914) If the inputs are considered as discrete events and a single inhibitory input vetoes excitatory inputs the neuron has traditionally been modelled as a logic-gated circuit. (McCulloch and Pitts, 1943) Although there is evidence that some axons can transmit subthreshold action potentials in addition to the traditional "all or none" action potentials, (Clark and Hausser, 2006) to our knowledge this analogue axonal transmission has not been described in RGCs. This analogue-digital neuronal computation is energetically costly, with the synapses responsible for the largest portion of the neuronal energy demands. (Harris et al., 2012) Using a genetically-encoded luminescent ATP reporter in cultured hippocampal neurons, Rangaraju *et al.* found that ATP synthesis in presynaptic boutons is coupled to activity, and that both glycolysis and OXPHOS are upregulated by neuronal activity and are required for the synaptic vesicle cycle, a major consumer of presynaptic ATP. (Rangaraju et al., 2014)

There is evidence that OXPHOS is particularly important to RGC dendrites. This is indicated by the intensive O_2 consumption in the IPL (Yu and Cringle, 2001) and the mitochondrial content in this region. We have recently shown that in vascularized retinas (marmoset and rat) the IPL displays intense punctate immunoreactivity for mitochondrial proteins. (Chidlow et al., 2019) Conversely, in the avascular retina (rabbit and guinea pig), intense labeling of photoreceptor inner segments was observed, but the inner and OPL display only weakly punctate staining, indicating that avascular retinas are generating ATP via non-aerobic glycolytic mechanisms. Enzyme histochemistry assays for three mitochondrial enzymes were also consistent with this pattern. (Chidlow et al., 2019)

4.2.3   Energy metabolism of RGC axons

Energy in RGC axons is largely consumed by generating action potentials and re-establishing the resting membrane potential, (Harris and Attwell, 2012) and is likely to be a critical evolutionary force influencing neuronal structure and function. (Crotty et al., 2006) The lack of saltatory conduction in the unmyelinated intraocular portion of the RGC axons places a particular bioenergetic burden on this component, and there is evidence that relationships between spatial limitations and energy demands influence the bioenergetics in RGC axons.

Perge *et al.* determined that mitochondrial volume predicts oxidative capacity and that the law of diminishing returns applies to RGC axons: twice the information rate requires more than twice the space and energy capacity. (Perge et al., 2009) Perge *et al.* provide evidence that the optic nerve conserves space and energy by transmitting most information at low rates over small-diameter axons with small terminal arbors whilst sending some information at higher rates over larger-diameter axons with larger terminal arbors. (Perge et al., 2009)

The trafficking and distribution of mitochondria within RGC axons indicates the importance of OXPHOS as an ATP generator for information transmission. The pattern of mitochondrial concentration in the unmyelinated segments resembles that of the myelinated segments, but for fibers thicker than 0.7 μm, the volume fraction is twofold greater. (Perge *et al.*, 2009) These calculations were performed on guinea pig optic nerve and conceivably the avascular guinea pig retina may not extrapolate to vascularised retinas; however, our own data suggest that the RGC somata and axons share a similar mitochondrial profile in both vascular and avascular retinas. (Chidlow et al., 2019) Furthermore, using transmission electron

microscopy, Wang *et al.* demonstrate that the unmyelinated portion of the RGC axons in primates (including humans) display varicosities rich in mitochondria that likely serve local high-energy demands of unmyelinated fibres. (Wang et al., 2003) In the optic nerve the unmyelinated prelaminar and laminar regions are rich in both cytochrome c oxidase and succinate dehydrogenase; however, myelination of fibres as they exited the lamina cribrosa is associated with an abrupt reduction in enzyme activity. (Andrews et al., 1999)

There is evidence that space limitations may dictate mitochondrial energy supply in RGCs. Harris and Attwell calculated that mitochondria alone are sufficient to supply the ATP demands in thicker axons but may not be sufficient in axons < 0.76 μm. (Harris and Attwell, 2012) In humans, normal optic nerve axon mean diameter ranges from 0.1-8.3 μm, (Jonas et al., 1990) suggesting that the smaller axons may require ATP supply via glycolysis in addition to OXPHOS.

To fuel the CAC, there is considerable evidence that oligodendrocytes export lactate (or pyruvate) via MCT1 to the periaxonal space and that the substrate is taken up by MCT2 transporters on the axolemma of myelinated CNS axons. (Funfschilling et al., 2012; Harun-Or-Rashid et al., 2018; Lee et al., 2012) MCT1 is highly enriched within oligodendroglia and its disruption causes neurodegeneration in animal and cell culture models. (Lee et al., 2012) Furthermore, compound action potentials (CAPs) in isolated aglycaemic optic nerves can be maintained by lactate. (Brown et al., 2003) Using a transgenic mouse with a fluorescent ATP-sensor, Trevisiol *et al.* measured ATP levels in the optic nerve as a function CAP. (Trevisiol et al., 2017) They demonstrated that high frequency stimulation caused a reduction in CAP generation with a corresponding reduction in ATP. They also noted that axonal ATP required both glycolytic and mitochondrial support and that even when glucose is abundant, lactate is an important additional fuel for ATP generation. (Trevisiol et al., 2017)

Recently, Gilley and Coleman, determined that nicotinamide mononucleotide adenylyltransferase 2 (Nmnat2) was a critical survival factor for axons. (Gilley and Coleman, 2010) This short-half-life, cytosolic enzyme is expressed in RGCs and catalyses an essential step in the NAD synthesis. There is evidence that the protective effect of Nmnat2 is afforded by a local bioenergetic mechanism. (Wang et al., 2005)

4.3 Vulnerability of RGCs to bioenergetic compromise

4.3.1 Evidence from animal models

High IOP-induced ocular ischemia in rats was originally described by Smith and Baird in 1952 (Smith and Baird, 1952) and reinvented by Buchi *et al.* in 1991. (Buchi et al., 1991) In this method, the intraocular pressure (IOP) is elevated above ocular perfusion pressure for a defined period, producing global ischemia with obstruction of both the retinal and uveal circulation, as evidenced by flattening of the ERG, whitening of the fundus and iris pallor. The histopathological features depend on the duration of exposure; however, in our hands 60-75 minutes of ischaemia produces pathology similar to central retinal artery occlusion, with sparing of the outer retina. The scotopic ERG b-wave is attenuated immediately by high IOP-induced ischemia and flattens within minutes. Bui *et al.* showed in rats that the inner retina derived scotopic threshold response (STR) was more sensitive to acute IOP elevation than ERG components arising from photoreceptors (a-wave) and bipolar cells (b-wave). (Bui et al., 2005) The lab of Crowston *et al.* previously determined the electroretinographic response as a function of IOP in mice. (Kong et al., 2009) The rate of functional recovery was assessed for 60 minutes after an IOP spike of 50 mm Hg for 30 minutes. During and immediately after IOP elevation, scotopic ERG signals were recorded in response to dim and bright flashes and analyzed for photoreceptoral (a-wave), ON-bipolar (b-wave), oscillatory potentials (OPs), and scotopic threshold responses (positive [p]STR/negative [n] STR) indicative of RGC function. (Sieving et al., 1986) The

pSTR was most sensitive to IOP elevation with 50% amplitude loss at 41 mm Hg. pSTR was significantly more sensitive than the b-wave, a-wave and OPs.

The permanent bilateral carotid occlusion (2VO) model in rats, which also markedly reduces both retinal and uveal flow, produces a rapid onset, profound injury to the proximal optic nerve, initially sparing the whereas the RGC somata and their unmyelinated axons. (Chidlow et al., 2010) Fast axonal transport is disrupted within 6 hours, damage to the axonal cytoskeleton in the proximal optic nerve detectable by 24 hours, and complete axonal loss within the infarcted area manifest within 3 days. Wallerian degeneration of the distal segment of the optic nerve proceeds thereafter, with almost complete loss of the optic nerve axonal cytoskeleton evident by 30 days. The outer retina remains relatively preserved. (Chidlow et al., 2010)

The high-pressure ischaemia model (which ceases both retinal and choroidal circulation) also characteristically injures the inner retina to a much greater extent than the outer retina.(Hughes, 1991) The reason for the relative sparing of the outer retina compared to the inner retina in rodent animal models that create a global reduction in ocular blood flow is unclear. One study has reported that this pattern is reversed in primates; (Parrish et al., 1982) however, to our knowledge, this has never been confirmed in a repeat study. The situation is further muddied by noting that both the 2VO model and the high IOP model in rats cause RGC axonal injury (Chidlow et al., 2011; Holman et al., 2010) with an unknown degree of primary injury to the RGC somata. Clinically, we note that an interruption in retinal blood supply for short periods causes an inner retinal infarction, but that photoreceptors can be separated from their blood supply for extended periods and still retain function once re-attached. Whether this remarkable ability of the photoreceptors relates to metabolic adaptability, judicious use of subretinal energy substrates or some other phenomenon is unknown. The intrinsic bioenergetic vulnerability of retinal cell types remains an area for further study.

These findings are consistent with those of Noell who compared electrophysiological responses from the retina and optic nerve in various species (including self-experimentation on a human subject) under conditions of anoxia. (Noell, 1951) He concluded that in man, the RGCs and their axons were the most susceptible. Our previous stoichiometric-based calculations indicate that the RGC oxygen requirements to maintain visual perception exceed the photoreceptors by at least a factor of 5, a finding consistent with the empirical data.

Animal models of glaucoma may produce an element of retinal and optic nerve ischemia. This is not necessarily an undesirable property and has, in fact, been the direct aim of some models.(Cioffi and Sullivan, 1999) In our hands, the translimbal laser-induced elevated IOP model in rats (Levkovitch-Verbin et al., 2002) produces a variable degree of axon transport disruption and pimonidazole labelling that correlates weakly with the degree of IOP elevation. Jassim and Inman have recently observed hypoxic elements after 4 weeks of IOP elevation in micobead murine model; however, the temporal profile of the hypoxia did not directly mirror the loss of RGCs. (Jassim and Inman, 2019) It is also important to note that many independent groups have demonstrated significant RGC degeneration after short-term IOP elevation using bead preparations with IOP levels well below those considered to impair retinal perfusion; hence, there, is clearly an important non-ischaemic component to these models at the level of the ONH.(El-Danaf and Huberman, 2015; Ito et al., 2016; Risner et al., 2018)

4.3.2   Anatomical and functional factors

The axons are subject to kinking and considerable stress and they pass through the lamina cribrosa. Morgan *et al.* noted that approximately 10% of axons had a tortuous path through the cribrosal plates and would be selectively vulnerable to compression of in diseases such as glaucoma. (Morgan et al., 1998)

 In unmyelinated axons, action potential propagation requires activation of voltage-gated sodium channels along the entire length of the axon, whereas action potential propagation along myelinated axons requires activation of voltage-gated sodium channels only at the nodes of Ranvier. (Hodgkin and Huxley, 1952) For optical reasons the intraocular RGC axons are unmyelinated in the retinal nerve fibre bundle and require relatively more energy to maintain action potentials than the saltatory conduction in the myelinated portion outside the globe. Based on calculations from data pertaining to the rat optic nerve axons, Harris and Attwell estimate that per action potential, each myelinated axon uses 23% of the ATP consumed by unmyelinated axons. (Harris and Attwell, 2012) The concept that unmyelinated axons require more energy is consistent with the finding on electron microscopy in monkeys demonstrating that mitochondria are concentrated in the prelaminar and laminar regions (Minckler et al., 1976) Similarly, histochemical and immunohistochemical evidence indicates that mitochondrial enzyme activity and immunoreactivity is higher in these unmyelinated regions. (Andrews et al., 1999; Barron et al., 2004; Bristow et al., 2002) Interestingly, one of us (JGC) has observed the preservation of myelinated nerve fibres in a patient with advanced glaucomatous axonal loss. (Toh et al., 2011)

In addition to the burden induced by lack of myelination in the intraocular portion of the optic nerve, the RGCs are an exception to the "wiring economy principle". (Raj and Chen, 2011) This principle postulates that, for a given wiring diagram, neurons are arranged in an animal to minimize the wiring cost. (Raj and Chen, 2011) The evolutionary cost can be attributed to various factors, including metabolic expenditures associated with signal propagation and maintenance. (Raj and Chen, 2011) Human RGCs are an exception to this principle due to anatomical and functional evolutionary priorities: to retain predatorial vision with forward-positioned eyes whilst accommodating our large forebrains, the RGC axons must extend approximately 11 cm from the soma to their first synapse in the lateral geniculate body.

4.3.3   Evidence from mitochondriopathies

Leber's hereditary optic neuropathy (LHON) results from base pair mutations in mitochondrial DNA causing dysfunction of Complex I in the ETC. Although the disease affects mitochondria in all cells, generally the genetic mutation only manifests in the RGCs, causing optic nerve degeneration and usually profound sequential loss of vision in both eyes. Although there is no clear explanation for the exclusivity of RGC pathology in LHON, its occurrence implies an exquisite sensitivity to impairment of OXPHOS. (Ito and Di Polo, 2017)

Approximately 75% of individuals with autosomal dominant optic atrophy have mutations in *OPA1*, a gene encoding a dynamin-related protein in the inner mitochondrial membrane that regulates mitochondrial dynamics. (Alexander et al., 2000) In a similar manner to LHON, OPA1 is ubiquitously expressed, but only RGCs manifest pathology. (Ito and Di Polo, 2017) Furthermore, OPA1 deficiency impairs OXPHOS efficiency, but compensation through increases in the distal complexes of the respiratory chain may preserve mitochondrial ATP production in patients who maintain normal vision. (Van Bergen et al., 2011) Williams *et al.* have demonstrated the presence of dendritic pruning in ON-centre RGCs in the $Opa1^{+/-}$ mouse model of autosomal dominant optic atrophy, (Williams et al., 2010) and that Opa1 is essential for RGC synaptic architecture and connectivity. (Williams et al., 2012) We note that an apparent mitochondrial sensitivity causing structural changes to the ON-centre RGCs in the inner sublamina of the IPL is not entirely consistent with O2 tension data observing lower O2 profiles in sublamina b; however, it is possible that the ON-centre RGCs are intrinsically more sensitive to mitochondrial impairment. These results highlight the

importance of normal mitochondrial fusion balance, as influenced by the OPA1 protein in maintaining the dendritic morphology of RGCs. (Williams et al., 2010)

5 GLAUCOMA

Glaucoma refers to a group of ocular conditions united by an IOP-associated, clinically characteristic optic neuropathy. (Casson et al., 2012b) Pathologically, glaucoma is characterised by a loss of all RGC compartments: somata, axons and dendrites. The overwhelming clinical impression is that the optic nerve head is the site of primary pathology. This observation is supported by evidence from primate models (Quigley and Anderson, 1977), human pathological studies (Quigley et al., 1981), and more recently in rodent models.(Chidlow et al., 2011; Howell et al., 2007) We have shown that the earliest indication of RGC damage is accumulation of proteins, transported by orthograde fast axonal transport within axons in the optic nerve head, which occurred as soon as 8 h after induction of glaucoma and was maximal by 24 h. Axonal cytoskeletal abnormalities were first observed in the ONH at 24 h. In contrast to the ONH, no axonal cytoskeletal damage was detected in the entire myelinated ON and tract until 3 days. (Chidlow et al., 2011)

Wallerian degeneration is the neurodegeneration of axons distal to the site of injury and is an important pathological feature in human (Quigley et al., 1981; Vrabec, 1976) and experimental glaucoma.(Chidlow et al., 2011; Conforti et al., 2007; Howell et al., 2007; Quigley and Anderson, 1977) The Wallerian degeneration slow allele (*Wld^S*) is a chimera of *Ube4b* and *Nmnat1* producing a fusion protein, WLD^S.(Mack et al., 2001) Expression of the WldS allele robustly protects synapses, dendrites, soma, and axons during glaucomatous insults (in genetic and inducible animal glaucoma models) (Harder et al., 2017; Howell et al., 2013; Williams et al., 2017a)

All forms of glaucoma, except so-called normal tension glaucoma (NTG), are associated with an elevated IOP at some point in the disease process, and IOP reduction is currently the only clinically proven strategy to reduce the rate of neurodegeneration, including in NTG. (Casson et al., 2012b; Collaborative Normal-Tension Glaucoma Study Group, 1998) The most common subtype is primary open-angle glaucoma (POAG). POAG is a genetically heterogenous group of diseases with a converging phenotype; some causative genes are implicated at the level of the aqueous outflow and others at the level of the RGCs. (Craig et al., 2020; Gharahkhani et al., 2014; MacGregor et al., 2018) The dominant risk factors for POAG are elevated IOP and increasing age, and although the pathogenesis of POAG remains unclear, there is a consilience of evidence indicating that impaired bioenergetics at the level of the RGC is an important causative factor. Bioenergetics in POAG may be impaired either directly via intrinsically aberrant energy metabolism or indirectly via impaired delivery of energy substrates.

5.1 Impaired Bioenergetics in POAG

5.1.1 Vascular Theory of Glaucoma

The concept that energy substrate delivery may be impaired in some forms of glaucoma is consistent with the vascular theory of glaucoma. The possible role of impaired blood flow to the optic nerve as cause of POAG has been considered for over 160 years. (Jaeger, 1858) Since this time, a plethora of evidence has accumulated, indicating that in at least some individuals with glaucoma and especially NTG, the blood flow to the optic nerve head and retina is impaired. (Flammer et al., 2002) The vascular theory considers glaucomatous optic neuropathy (GON) to be a consequence of insufficient blood supply due to either increased IOP or other factors reducing ocular blood flow, (Flammer, 1994) including vascular dysregulation. (Flammer et al., 2002)

Ocular perfusion pressure (OPP) is not easily directly measurable, and the difference between blood pressure and IOP has been suggested as a surrogate of OPP in epidemiological studies. (Tielsch et al., 1995) There have been numerous population-based studies reporting an association between ocular perfusion pressure and POAG. (Leske, 2009; Leske et al., 2008; Memarzadeh et al., 2010) However, the statistical analysis in these studies has commonly used a multivariate analysis with a surrogate predictor of OPP that includes IOP in its calculation. (Leske, 2009) Khawaja astutely cautions that this approach is mathematically flawed and that no conclusions about OPP independent of IOP can logically be drawn. (Khawaja et al., 2013)

Notwithstanding the statistical flaws pertaining to the epidemiological data, there is nevertheless abundant data from a variety of techniques indicating that blood flow to the retina, choroid, and optic nerve is impaired in at least some individuals glaucoma. (Flammer et al., 2002) Recently, these data have been further supported by evidence of impaired retinal and optic nerve head blood flow using optical coherence tomography angiography, (Werner and Shen, 2019) a feature that is being increasingly utilized to detect early disease. (Hou et al., 2020) In NTG, there is additional evidence that the blood flow dysregulation is not restricted to the eye. (Drance et al., 1988; Flammer et al., 2002) Cold-induced vasospasm of the extremities has been reported to be associated with the "focal ischemic" type of GON, whilst the "senile sclerotic disc" phenotype is reportedly associated with cardiovascular risk factors. (Broadway and Drance, 1998; Geijssen and Greve, 1987; Nicolela and Drance, 1996) Furthermore, cardiovascular disease has been reported as a significant risk factor for rapid glaucoma progression irrespective of IOP. (Chan et al., 2017)

5.2   Intrinsic Bioenergetic Impairment in Glaucoma

There is considerable evidence for mitochondrial impairment in animal models of glaucoma and human glaucoma. In DBA/2J mice with early glaucoma there is differential expression of genes encoding mitochondrial proteins, and significant enrichment of genes in the mitochondrial dysfunction and oxidative phosphorylation pathways, including enrichment of signal transcripts promoting redox homeostasis. (Williams et al., 2017b) In addition, mitochondrial fission unfolded protein response (UPRmt) genes were also differentially expressed, and electron microscopy (EM) revealed abnormal mitochondria with reduced cristae volume in the dendrites of RGCs, but not in those of control RGCs. (Williams et al., 2017b)

Van Bergen *et al.* reported that, compared to age-matched controls, Complex-I enzyme specific activity was reduced by 18% in lymphoblasts from individuals with POAG compared with a 29% reduction in individuals with LHON. (Van Bergen et al., 2015) In addition, multiple mitochondrial DNA abnormalities have been detected in individuals with POAG, with associated deficits in mitochondrial respiratory activity. (Abu-Amero et al., 2006) Furthermore, recent evidence indicates that mitochondrial DNA ancestral lineages modulate the risk for primary open-angle glaucoma in populations of European descent. (Singh et al., 2018) These data suggest that POAG could be conceptualized as an age-exacerbated mitochondriopathy. (Lee et al., 2011)

In the DBA/2J mouse model of glaucoma, the amplitude and the integral of the optic nerve CAPs decreased considerably by 6 months of age as a function of increasing IOP levels. (Baltan et al., 2010) In this model, at young ages, elevated IOP was directly associated with increased vulnerability to impaired energy substrate supply, and at older ages there was a differential loss of CAPs in small, slow conducting axons associated with a declining metabolic reserve. (Baltan et al., 2010) This is consistent with the calculations by Harris & Attwell indicating that small-diameter fibres may have insufficient space for mitochondria to maintain ATP supply. (Harris and Attwell, 2012; Yokota et al., 2015)

Motor proteins (kinesins) on microtubule tracks deliver proteins, mitochondria and other essential cargoes to the distal synapse: this process constitutes anterograde axonal transport. This is an energy dependent process and energy deficit is an important cause of axonal transport failure. (Millecamps and Julien, 2013)

Mitochondria are produced in the soma and actively shuttled and positioned to meet the localized needs of the cell. (Sajic et al., 2013) They are delivered and retrieved with their average velocity falling between that of fast-moving small vesicles and slow-moving cytoskeletal proteins. (Grafstein and Forman, 1980)) because they are frequently stationary.

Elevated IOP in rodents (Chidlow et al., 2011) and primates (Quigley et al., 1979; Radius and Anderson, 1981) interrupts axonal mitochondrial transport. Elegant intravital multiphoton imaging of mouse RGCs in vivo have shown that the mitochondrial transport is highly dynamic under physiological conditions but is impaired in a murine model of chronically elevated IOP, particularly in older mice. (Takihara et al., 2015)

Williams *et al.* reported a comprehensive sequence of experiments on the DBA/2J mouse which indicated that retinal NAD^+ levels decline with age which is exacerbated in glaucomatous animals. (Williams et al., 2017b) (Williams et al., 2018; Williams et al., 2017c) This is consistent with the earlier finding that Nmnat2 was a critical survival factor for neurons, (Chidlow et al., 2017) and suggests that NAD-related energy metabolism is critical for RGC axons and is impaired in glaucoma.

5.2.1 *Mitochondria and Reactive Oxygen Species (ROS)*

Like all physical processes, the ETC is not perfectly efficient: a portion of electrons leak from complexes I-III and react with oxygen to form the superoxide radical. (Turrens, 2003) Carrying an unpaired electron, superoxide is a potent oxidant and the shift in the redox status of a cell in favour of oxidants is termed oxidative stress with damaging effects on fundamental cellular components, including proteins, DNA and lipids. Hence, the mitochondria are a major cellular source of ROS. (Turrens, 2003) Electrons are transferred to NAD^+ in the CAC; hence increased $NADH/NAD^+$ exacerbates mitochondrial ROS production. In addition, genetic dysregulation of OXPHOS can increase ROS production, damaging mitochondria in a positive feed-back cascade. There is an increasing body of clinical as well as experimental evidence that oxidative stress contributes to the pathology of glaucoma. (Tezel, 2006) Given the association of mitochondrial failure with increased oxidative stress, a mitochondria-targeted neuroprotection strategy is appealing from the perspective of both ATP supply and ROS reduction.

6 BIOENERGETIC-BASED THERAPY IN GLAUCOMA

6.1 Principles of Neuroprotection in Glaucoma

Although there is likely a continuum of neuronal health status, for strategic purposes we conceptualize a tripartite categorization: neurons are either healthy, sick, or dead. Neuroprotection is broadly defined as a relative protection of neurons against an actual or threatened insult. (Casson et al., 2012a) Dead neurons are not amenable to neuroprotection, and the focus of therapeutic strategy is on sick or threatened neurons (arguably due to the vulnerable state of RGCs, they are always under threat). In the case of an ongoing chronic neurodegenerative insult, such as POAG, the relative preservation of neuronal integrity implies a reduction in the rate of neurodegeneration over time. (Casson et al., 2012a) A related concept is neurorecovery, defined as the complete or partial restoration of a living, non-functioning or poorly functioning neuron to structural and functional health. (Casson et al., 2012a) Conceivably, a strategy could provide neurorecovery in the short term but not neuroprotection over time; however, for the more likely situation that a neurorecovery strategy also proves to be neuroprotective, we have proposed the term neurorescue. (Casson et al., 2012a)

Our aim in introducing these terms in the literature was to promote the concept of relatively inexpensive short duration clinical trials of novel therapies that demonstrated neurorecovery in glaucoma providing motivation for longer duration, more costly trials investigating neuroprotection. We additionally aimed to investigate potential therapies that satisfied the principles of neuroprotection: (1) primarily affected neurons are targeted; (2) the therapy protects all neuronal compartments; (3) upstream death pathways

are addressed. (Casson et al., 2012a) The fundamental requirement of energy to maintain structural and functional integrity of all RGC compartments and evidence that energy impairment is an important pathogenic factor in at least some forms of glaucoma provides strong motivation for the strategy of manipulating energy metabolism as a therapeutic approach to glaucoma. (Schober et al., 2008)

6.2   Animal Studies

6.2.1   Glucose

In 1972, Weiss, using a pressure-induced ischemia model in rabbits, found that in the first 20 minutes of ischemia, retinal glycogen was depleted, and after this period the vitreous became an important source of glucose for anaerobic glycolysis. (Weiss, 1972) Weiss concluded that the vitreous glucose was the most important energy substrate for retinal ischemia lasting more than 20 minutes and that the exhaustion of anaerobic glycolysis was a crucial factor in determining the ischemic tolerance time of the rabbit retina. (Weiss, 1972) In 2004, we hypothesized that supplying additional glucose to the vitreous would attenuate ischaemic retinal injury. We reported the striking neuroprotective effect of an elevated vitreous glucose level against an acute, high-IOP induced ischemic retinal insult. (Casson et al., 2004) We subsequently demonstrated the reverse, namely that reducing the vitreous glucose concentration exacerbated ischemic retinal injury (Casson et al., 2004). In subsequent studies, we revealed that the protective effect of glucose was not restricted to acute paradigms of injury: an elevated vitreous glucose level protected against RGC degeneration in a rat model of chronic hypoperfusion (Holman et al., 2010) as well as in a laser-induced model of glaucoma. (Ebneter et al., 2011) Chronic elevation of the vitreal glucose concentration within a clinical setting is obviously not desirable, but these studies demonstrate proof-of-principle that energy-deprived RGCs can benefit from energy substrates contained within the vitreous reservoir.

6.2.2   Nicotinamide

Success with this basic approach motivated further bioenergetic research, and, in 2008, Osborne and co-workers reported that nicotinamide attenuated experimental ischemic retinal injury. (Ji et al., 2008) Recently, Williams *et al.* noted significant age-related declines in NAD^+ in the DBA/2J mouse model of glaucoma and hypothesized that increasing NAD^+ levels would protect against glaucomatous changes by decreasing the probability of metabolic/energetic failure and rendering the RGCs more resilient to IOP-induced stress. (Williams et al., 2017b) To test this hypothesis, they performed a comprehensive set of experiments, showing that oral supplementation with nicotinamide (NAM; a precursor of NAD^+ and the amide of vitamin B_3), resulted in a robust neuroprotection of RGCs and their axons. This result is particularly appealing because of the relative safety of clinical translation. At a moderate dose, equating to approximately 3 g/d for a 70 kg human, (Nair and Jacob, 2016) the vitamin B_3 supplementation was highly effective, and became almost completely protective at a high dose level, (equating to approximately 11.4 g/d for a 70 kg human). Importantly, this treatment also protected against two other glaucoma-relevant insults; axotomy (the destruction of the RGC axon; a key component in glaucoma) and TNF-α induced neuroinflammation (*TNF* polymorphisms have been demonstrated in glaucoma patients). Williams *et al.* further demonstrated that gene therapy (driving expression of *Nmnat1*, a key NAD^+ producing enzyme) was similarly neuroprotective.

6.2.3   CoQ$_{10}$

CoQ10 is a component of the mitochondrial respiratory pathway, carrying electrons from complexes I and II to complex III, and is a potent antioxidant. Oral administration of coenzyme Q_{10} has been shown to attenuate striatal lesions produced by systemic administration of 3-nitropropionic acid and significantly increased life span in a transgenic mouse model of familial amyotrophic lateral sclerosis. (Matthews et al., 1998) The neuroprotective effect of CoQ$_{10}$ has also been demonstrated in retinal ischemic and experimental glaucoma models. (Nucci et al., 2007) (Davis et al., 2017; Lee et al., 2014a)

6.2.4 Creatine kinase

There are two main isoforms of creatine kinase: cytosolic creatine kinase that balances energy distribution in the cytosol, and mitochondrial creatine kinase that buffers energy between the mitochondria and the cytosol. Creatine supplementation, which results in increased levels of phosphocreatine, may provide neuroprotection through greater energy buffering, enhancing blood flow (Prass et al., 2007)and reducing glutamate toxicity via enhanced phosphocreatine-dependent glutamate uptake by synaptic vesicles. (Xu et al., 1996) Creatine supplementation has provided significant neuroprotection against *in vivo* models of traumatic brain injury, (Sullivan et al., 2000) cerebral ischemia, (Zhu et al., 2004) amyotrophic lateral sclerosis (Klivenyi et al., 1999), and Huntington's disease. (Ferrante et al., 2000) We recently reported that creatine significantly prevented retinal neuronal death caused by sodium azide and NMDA *in vitro* (Fig. 9). Curiously, however, creatine was not protective in *in vivo* models of NMDA-induced RGC death or high-IOP induced ischemia-reperfusion. (Sia et al., 2019) The explanation underlying this discrepancy is not readily apparent, but may conceivably relate to an inadequate dose of creatine reaching RGCs, or perhaps reflect suboptimal uptake of creatine by its transporter. It will be important to test creatine supplementation in chronic, rather than acute, models of RGC death.
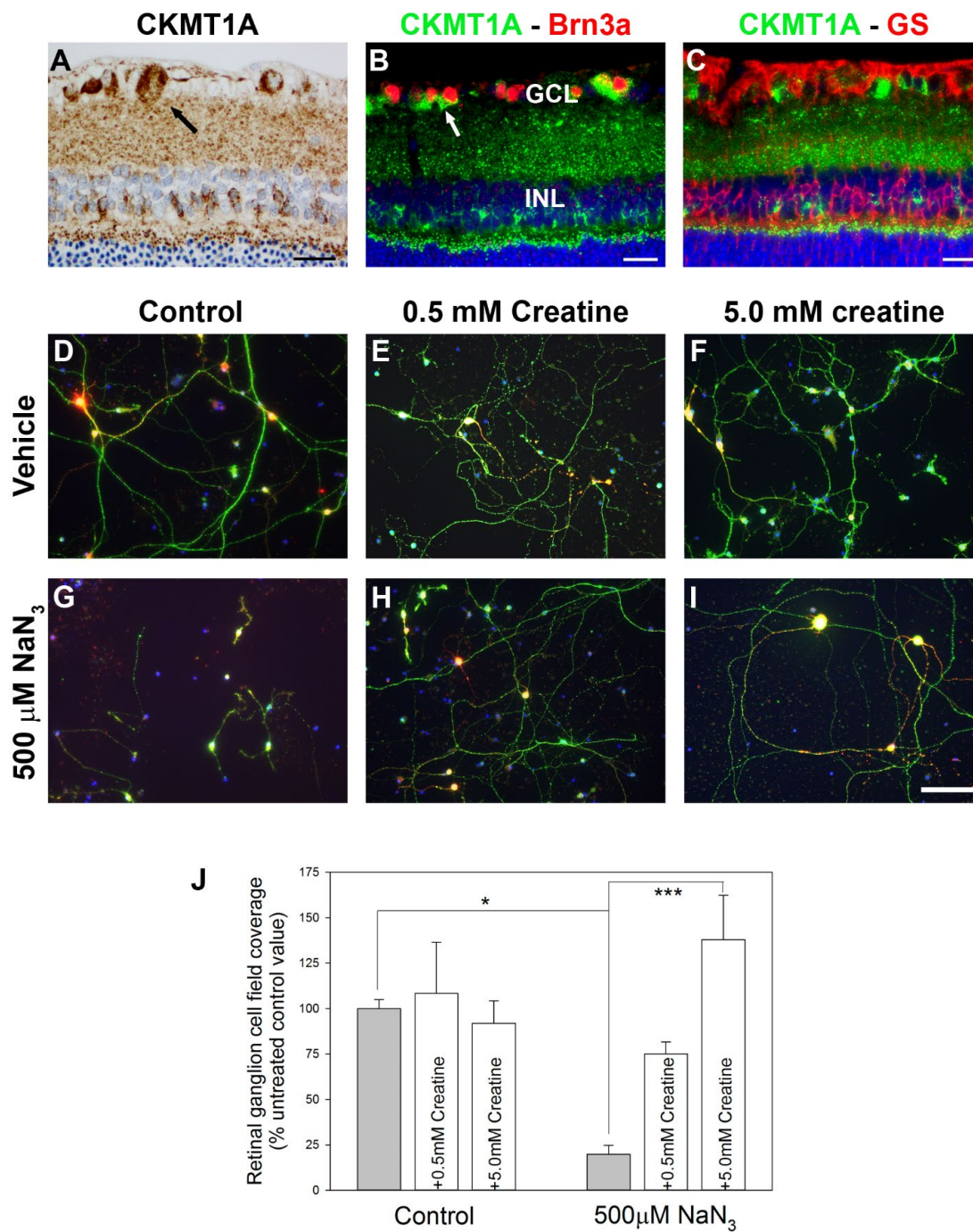
Figure 9: Expression of ubiquitous mitochondrial creatine kinase (CK-MT1A) in rat retina. (A-C) Immunolabelling was intense in both plexiform layers and in perikarya in the GCL (A, arrow). Double-labeling immunofluorescence revealed colocalization of CK-MT1A with the retinal ganglion cell marker Brn3a (B), but not with the Müller cell marker glutamine synthetase (GS; C).

(D-J) Protective effect of creatine against toxicity induced to RGCs in culture by sodium azide (NaN$_3$; 500 μM). RGCs were treated with NaN$_3$ in the presence or absence of creatine (0.5 mM, 5.0 mM) for 24 hours and subsequently fixed and labelled for tau (green; axons) and MAP2 (red; dendrites). NaN$_3$ induced widespread damage to RGCs including loss of dendrites, the shortening and destruction of axons and the reduction in cell numbers (G). This was significantly ameliorated in the presence of creatine when applied at both 0.5 mM (H) and 5.0 mM (I). These data clearly show that creatine is able to protect RGCs in culture from metabolic compromise induced by the mitochondrial Complex IV inhibitor, NaN$_3$.

*** $P < 0.001$; * $P > 0.05$ when comparing data derived from creatine-supplemented cells with NaN_3-treated cells alone, by one-way ANOVA followed by Tukey multiple comparisons test (n = 6 determinations per treatment).

Scale bars: A = 25 µm; B, C = 20 µm; D-I = 40 µm. GCL, ganglion cell layer; INL, inner nuclear layer.

6.2.5   Pyruvate

The finding of high levels of MPC 1 and PDH, as well as the LDHB isoform, in RGCs indicate that pyruvate is potentially an excellent energy substrate for RGCs that may be synergistic with vitamin B_3. *In vitro,* we have recently demonstrated that pyruvate rescues RGCs from both glucose deprivation-induced death and oxidative injury. (Williams et al., 2020) We have also shown that oral pyruvate supplementation has a robust neuroprotective effect in both the DBA/2J mouse and the laser-induced rat model of glaucoma. (Williams et al., 2020) Furthermore, pyruvate and nicotinamide exhibit neuroprotective synergy in the DBA/2J model. (Williams et al., 2020)

6.2.6   mTOR

mTOR (mammalian target of rapamycin) is a serine/threonine protein kinase that has been shown to have roles in cell growth, development and survival, as well as in response to upstream events including growth factors, hormones, DNA damage and energy metabolites. (Hwang et al., 2008; Jewell and Guan, 2013) Translational control by mTOR has been shown to be essential for neuronal and synaptic plasticity. (Buffington et al., 2014) Failure of neuronal compartments to regenerate is the major barrier that prevents recovery from CNS injury and the failure for the optic nerve to regenerate has been linked to axotomy-induced RGC death. Given the mTOR pathway's role in the CNS this makes mTOR activation an attractive candidate for neuronal recovery following retinal injury.

Recent insights show a promising role for mTOR activation in neuronal regeneration following injury. Using an optic nerve crush model Park *et al.*, showed that a deletion of PTEN or TSC1 (negative regulators of mTOR) led to axonal recovery following optic nerve crush showing the importance for the regulation of the mTOR pathway in intrinsic regrowth responsiveness. (Park et al., 2008) In studies by Morquette *et al.*, a role for the mTOR in RGC dendrite degeneration following optic nerve crush was shown. (Morquette et al., 2015) mTOR was markedly decreased in RGCs which correlated with dendritic degeneration. Using siRNA against REDD2 (an mTOR repressor) stimulated mTOR activity in RGCs and lead to an increase in the integrity of dendritic architecture. Treating eyes with rapamycin (an mTOR inhibitor) following this siRNA treatment blocked the effect of the REDD2 siRNA confirming that the response was due to the effect of mTOR. Stimulated mTOR activity was also potent at restoring glutamatergic synapses between bipolar cells and RGCs. (Morquette et al., 2015) Further supporting this, mTOR pathway activation occurs early in DBA/2J glaucoma, (Williams et al., 2017b) and axotomy-induced dendrite retraction triggers a loss of mTOR in RGCs. Recently published data from Agostinone *et al.* and unpublished research from the laboratory of PAW indicates that insulin-dependent activation of mTOR complex 1 robustly prevents glaucomatous degenerative events. (Agostinone et al., 2018)

RGC dendrites are dynamic integrators of synaptic input in the retina and undergo remodeling in human glaucoma (Tribble et al., 2019) Due to the absence of spines on RGC dendrites this remodeling is often limited to a reduction in dendritic integrity measured by an often-marked loss in synaptic numbers, a reduction in secondary and tertiary dendrites and general dendritic shrinkage. This is both evident in genetic models of disease and mechanical insults to retina and optic nerve.

In the brain, many studies have shown the balance of neuronal activity and neurotrophins in dendrite remodeling and there may be some key mechanisms that regulate dendritic maintenance. (Mironova and Giger, 2013) One of these candidates is the PI3K/Akt signaling pathway that, in combination with mTOR,

can regulate synaptic plasticity and induce neurite regrowth. (Dyer et al., 2016) This pathway is downstream of Ras and BDNF. The PI3K-Akt-mTOR pathway is efficient at the regulation of dendritic branching and morphology; inhibiting PI3K-Akt signaling reduces dendritic complexity and soma size whereas overexpressing PI3K or Akt lead to an increase in dendritic complexity. (Dyer et al., 2016) Applying rapamycin reduced dendritic size. Knockdown of mTOR using siRNA decreased dendritic branching in hippocampal neurons that was rescued by a rapamycin-resistant mutant of mTOR. (Urbanska et al., 2012) In addition, the well-characterized actions of BDNF on dendritic arborization are blocked by administration of rapamycin. (Urbanska et al., 2012) This implies that BDNF promotion of dendrite branching is partially mTOR dependent. Taken together, these data show that PI3K, Akt, and BDNF may act through mTOR to regulate dendritic complexity by modulating dendritic protein synthesis. This PI3K-Akt-mTOR pathway may well be a key signaling pathway in neuronal plasticity. Pharmacological agents that activate the mTOR pathway may be of therapeutic benefit in optic neuropathies as well as other neurodegenerative diseases.

6.3   Clinical studies

Bioenergetic-based neuroprotection with supplements such a vitamin B_3 and pyruvate, is particularly appealing because of the excellent safety profile of the agents. Furthermore, we have endeavoured to develop a strategy that optimizes translation and delivers novel effective therapies to patients as rapidly as possible. Relatively rapid demonstration of clinical neurorecovery, over a period of less than 6 months, motivates subsequent longer-duration trials with larger sample sizes. This approach requires clinical markers of neurorecovery. In a double-blind, randomized trial, we previously demonstrated that concentrated topical glucose can reach the vitreous cavity in pseudophakic individuals and that short-term intensive treatment can temporarily recover contrast sensitivity in some individuals with POAG. (Casson et al., 2014) We chose contrast sensitivity as a psychophysical biomarker because although it is not routinely measured in clinical practice, it is well known to be affected by glaucoma, (Hitchings et al., 1981) is an inexpensive non-invasive measure and had previously been shown to recover after IOP reduction (Gandolfi et al., 2005) and after brimonidine treatment for NTG. (Evans et al., 2003) This study was important because it demonstrated a proof-of-principle approach but was unlikely to be a viable strategy for a chronic glaucoma. Furthermore, it was important to develop alternative methods to measure RGC recovery.

Electrophysiological measurements of RGC provide an objective measure of function. The pattern electroretinogram (PERG) can isolate the RGC responses in animals and humans but is cumbersome to administer. (Arden et al., 1982; Ventura and Porciatti, 2006) Bui *et al.* have shown that both the positive and negative scotopic threshold response of the rat ERG depend directly upon intact GC responses, and that amacrine cell contributions to these components are relatively small. (Bui and Fortune, 2004) The photopic negative response (PhNR) is a corneal negative potential after the b-wave of the photopic ERG. There is good evidence that the PhNR is a manifestation of RGC spiking. One of us (JGC), has developed this tool as a marker of neurorecovery in animal models of glaucoma, demonstrating recovery after cessation of a limited IOP challenge. (Chrysostomou and Crowston, 2013) Recently, we have completed a double-blind, randomized cross-over study assessing the effect of oral vitamin B_3 supplementation on recovery of the PhNR in human POAG. (Hui et al., 2020) After 12 weeks of treatment, we found a significant enhancement of the PhNR response compared to baseline. An ongoing placebo-controlled trial at Columbia University (NCT03797469) is designed to assess the effect of a combination of vitamin B_3 and pyruvate on rate of change of visual field defects in glaucoma.

7 CONCLUSIONS AND FUTURE DIRECTIONS

The relatively large energy substrate demands make the retina vulnerable to energy insufficiency. In particular, evolutionary pressures to optimize human vision have been traded against RGCs' fragility. Details of the metabolic profiles of the different retinal cells remain poorly understood and are challenging to resolve. Detailed immunohistochemical mapping of the energy pathway enzymes and substrate transporters has provided some insights and highlighted interspecies differences. The different spatial metabolic patterns between the vascular and avascular retinas can account for some inconsistent data in the literature. There is a consilience of evidence that at least some individuals with glaucoma have impaired RGC energy metabolism, either due to impaired nutrient supply or intrinsic metabolic perturbations. Bioenergetic-based therapy for glaucoma has a compelling pathophysiological foundation and is supported by recent successes in animal models. Recent demonstrations of visual and electrophysiological neurorecovery in humans with POAG is highly encouraging and motivates longer duration trials investigating bioenergetic neuroprotection.

Clinical trials of bioenergetic neuroprotection are challenging due to the chronic nature of the disease, the variability in progression rates and the fact that patients are already receiving pressure-lowering therapy. Nevertheless, there is reason to be confident that the signal from an adjunctive, efficacious neuroprotectant would be discernible above background noise in a time frame within 2 years without requiring enormous sample sizes. The UK Glaucoma Treatment Study used an event-based outcome in visual field progression to demonstrate, within a 2-year period, that latanoprost significantly reduced the rate of defined progression compared to placebo. (Garway-Heath et al., 2015) In fact, a significant difference ($P < 0.05$) in the survival analysis between groups was reached by 12 months. This study performed analyses on approximately 230 patients in each group. The short duration of this study motivates similar trials assessing neuroprotectants. Bioenergetic neuroprotectants are particularly appealing because of their excellent safety profile. An alternative methodology would be to conduct a trend-based analysis on the rate of change of mean deviation (MD). De Moraes *et al*. note that a 30% decrease in rate of visual field progression can be reliably projected to have a significant effect on health-related quality of life. (De Moraes et al., 2017) In a clinic-based study from a tertiary care centre in Sweden, Heijl *et al.* report that progression rates varied considerably among patients with a mean of 0.80 dB ∕ year (SD 0.82). (Heijl et al., 2013) From a large clinic-based study in Portsmouth, Kirwan *et al.* reported that for those with an initial MD worse than −3 dB, 36.2% progressed at more than −0.5 dB/year and 5.7% progressed at more than −2 dB/year. (Kirwan et al., 2014) Predictors of rapid progression include worse initial MD, larger cup/disc ratios and older age. (Lee et al., 2014b) Hence, obtaining progressing patients on IOP-lowering therapy for a neuroprotection trial would not be problematic. We are planning a randomized clinical trial of vitamin B_3 supplementation in glaucoma based on these calculations.

References

Abu-Amero, K.K., Morales, J., Bosley, T.M., 2006. Mitochondrial abnormalities in patients with primary open-angle glaucoma. Investigative ophthalmology & visual science 47, 2533-2541.

Adrian, E.D., 1914. The all-or-none principle in nerve. J Physiol 47, 460-474.

Agostinone, J., Alarcon-Martinez, L., Gamlin, C., Yu, W.Q., Wong, R.O.L., Di Polo, A., 2018. Insulin signalling promotes dendrite and synapse regeneration and restores circuit function after axonal injury. Brain 141, 1963-1980.

Alexander, C., Votruba, M., Pesch, U.E., Thiselton, D.L., Mayer, S., Moore, A., Rodriguez, M., Kellner, U., Leo-Kottler, B., Auburger, G., 2000. OPA1, encoding a dynamin-related GTPase, is mutated in autosomal dominant optic atrophy linked to chromosome 3q28. Nature genetics 26, 211-215.

Ames, A., 3rd, Li, Y.Y., Heher, E.C., Kimble, C.R., 1992. Energy metabolism of rabbit retina as related to function: high cost of Na+ transport. J Neurosci 12, 840-853.

Andrews, R.M., Griffiths, P.G., Johnson, M.A., Turnbull, D.M., 1999. Histochemical localisation of mitochondrial enzyme activity in human optic nerve and retina. Br J Ophthalmol 83, 231-235.

Arden, G.B., Vaegan, Hogg, C.R., 1982. Clinical and experimental evidence that the pattern electroretinogram (PERG) is generated in more proximal retinal layers than the focal electroretinogram (FERG). Ann N Y Acad Sci 388, 580-607.

Baltan, S., Inman, D.M., Danilov, C.A., Morrison, R.S., Calkins, D.J., Horner, P.J., 2010. Metabolic vulnerability disposes retinal ganglion cell axons to dysfunction in a model of glaucomatous degeneration. J Neurosci 30, 5644-5652.

Barron, M.J., Griffiths, P., Turnbull, D.M., Bates, D., Nichols, P., 2004. The distributions of mitochondria and sodium channels reflect the specific energy requirements and conduction properties of the human optic nerve head. Br J Ophthalmol 88, 286-290.

Benner, S.A., 2010. Defining life. Astrobiology 10, 1021-1030.

Berg, J.M., Tymoczko, J.L., Stryer, L., 2012. Biochemistry. W.H. Freeman, Basingstoke.

Bernstein, M.H., Hollenberg, M.J., 1965. Fine structure of the choriocappillaris and retinal capillaries. Invest Ophthalmol 4, 1016-1025.

Bouzier-Sore, A.K., Serres, S., Canioni, P., Merle, M., 2003. Lactate involvement in neuron-glia metabolic interaction: (13)C-NMR spectroscopy contribution. Biochimie 85, 841-848.

Boycott, B.B., Wassle, H., 1991. Morphological Classification of Bipolar Cells of the Primate Retina. Eur J Neurosci 3, 1069-1088.

Bristow, E.A., Griffiths, P.G., Andrews, R.M., Johnson, M.A., Turnbull, D.M., 2002. The distribution of mitochondrial activity in relation to optic nerve structure. Arch Ophthalmol 120, 791-796.

Broadway, D.C., Drance, S.M., 1998. Glaucoma and vasospasm. Br J Ophthalmol 82, 862-870.

Brooks, G.A., 2018. The Science and Translation of Lactate Shuttle Theory. Cell Metab 27, 757-785.

Brown, A.M., Tekkok, S.B., Ransom, B.R., 2003. Glycogen regulation and functional role in mouse white matter. J Physiol 549, 501-512.

Buchi, E.R., Suivaizdis, I., Fu, J., 1991. Pressure-induced retinal ischemia in rats: an experimental model for quantitative study. Ophthalmologica 203, 138-147.

Buffington, S.A., Huang, W., Costa-Mattioli, M., 2014. Translational control in synaptic plasticity and cognitive dysfunction. Annu Rev Neurosci 37, 17-38.

Bui, B.V., Edmunds, B., Cioffi, G.A., Fortune, B., 2005. The gradient of retinal functional changes during acute intraocular pressure elevation. Invest Ophthalmol Vis Sci 46, 202-213.

Bui, B.V., Fortune, B., 2004. Ganglion cell contributions to the rat full-field electroretinogram. J Physiol 555, 153-173.

Calkins, D.J., Schein, S.J., Tsukamoto, Y., Sterling, P., 1994. M and L cones in macaque fovea connect to midget ganglion cells by different numbers of excitatory synapses. Nature 371, 70-72.

Campbell, J.P., Zhang, M., Hwang, T.S., Bailey, S.T., Wilson, D.J., Jia, Y., Huang, D., 2017. Detailed Vascular Anatomy of the Human Retina by Projection-Resolved Optical Coherence Tomography Angiography. Sci Rep 7, 42201.

Casson, R.J., Chidlow, G., Ebneter, A., Wood, J.P., Crowston, J., Goldberg, I., 2012a. Translational neuroprotection research in glaucoma: a review of definitions and principles. Clin Exp Ophthalmol 40, 350-357.

Casson, R.J., Chidlow, G., Han, G., Wood, J.P., 2013. An explanation for the Warburg effect in the adult mammalian retina. Clin Exp Ophthalmol 41, 517.

Casson, R.J., Chidlow, G., Wood, J.P., Crowston, J.G., Goldberg, I., 2012b. Definition of glaucoma: clinical and experimental concepts. Clin Exp Ophthalmol 40, 341-349.

Casson, R.J., Chidlow, G., Wood, J.P., Osborne, N.N., 2004. The effect of hyperglycemia on experimental retinal ischemia. Arch Ophthalmol 122, 361-366.

Casson, R.J., Han, G., Ebneter, A., Chidlow, G., Glihotra, J., Newland, H., Wood, J.P., 2014. Glucose-induced temporary visual recovery in primary open-angle glaucoma: a double-blind, randomized study. Ophthalmology 121, 1203-1211.

Casson, R.J., Wood, J.P., Han, G., Kittipassorn, T., Peet, D.J., Chidlow, G., 2016. M-Type Pyruvate Kinase Isoforms and Lactate Dehydrogenase A in the Mammalian Retina: Metabolic Implications. Invest Ophthalmol Vis Sci 57, 66-80.

Chan, T.C.W., Bala, C., Siu, A., Wan, F., White, A., 2017. Risk Factors for Rapid Glaucoma Disease Progression. Am J Ophthalmol 180, 151-157.

Chertov, A.O., Holzhausen, L., Kuok, I.T., Couron, D., Parker, E., Linton, J.D., Sadilek, M., Sweet, I.R., Hurley, J.B., 2011. Roles of glucose in photoreceptor survival. J Biol Chem 286, 34700-34711.

Chidlow, G., Ebneter, A., Wood, J.P., Casson, R.J., 2011. The optic nerve head is the site of axonal transport disruption, axonal cytoskeleton damage and putative axonal regeneration failure in a rat model of glaucoma. Acta neuropathologica 121, 737-751.

Chidlow, G., Holman, M.C., Wood, J.P., Casson, R.J., 2010. Spatiotemporal characterization of optic nerve degeneration after chronic hypoperfusion in the rat. Invest Ophthalmol Vis Sci 51, 1483-1497.

Chidlow, G., Wood, J.P.M., Casson, R.J., 2017. Investigations into Hypoxia and Oxidative Stress at the Optic Nerve Head in a Rat Model of Glaucoma. Front Neurosci 11, 478.

Chidlow, G., Wood, J.P.M., Sia, P.I., Casson, R.J., 2019. Distribution and Activity of Mitochondrial Proteins in Vascular and Avascular Retinas: Implications for Retinal Metabolism. Invest Ophthalmol Vis Sci 60, 331-344.

Chih, C.P., Lipton, P., Roberts, E.L., Jr., 2001. Do active cerebral neurons really use lactate rather than glucose? Trends Neurosci 24, 573-578.

Chinchore, Y., Begaj, T., Wu, D., Drokhlyansky, E., Cepko, C.L., 2017. Glycolytic reliance promotes anabolism in photoreceptors. Elife 6.

Chinopoulos, C., 2013. Which way does the citric acid cycle turn during hypoxia? The critical role of alpha-ketoglutarate dehydrogenase complex. J Neurosci Res 91, 1030-1043.

Christofk, H.R., Vander Heiden, M.G., Harris, M.H., Ramanathan, A., Gerszten, R.E., Wei, R., Fleming, M.D., Schreiber, S.L., Cantley, L.C., 2008. The M2 splice isoform of pyruvate kinase is important for cancer metabolism and tumour growth. Nature 452, 230-233.

Chrysostomou, V., Crowston, J.G., 2013. The photopic negative response of the mouse electroretinogram: reduction by acute elevation of intraocular pressure. Invest Ophthalmol Vis Sci 54, 4691-4697.

Cioffi, G.A., Sullivan, P., 1999. The effect of chronic ischemia on the primate optic nerve. Eur J Ophthalmol 9 Suppl 1, S34-36.

Clark, B., Hausser, M., 2006. Neural coding: hybrid analog and digital signalling in axons. Curr Biol 16, R585-588.

Clarke, D.D., Sokoloff, L., 1999. Circulation and Energy Metabolism of the Brain.

Collaborative Normal-Tension Glaucoma Study Group, 1998. The effectiveness of intraocular pressure reduction in the treatment of normal-tension glaucoma. . Am J Ophthalmol 126, 498-505.

Conforti, L., Adalbert, R., Coleman, M.P., 2007. Neuronal death: where does the end begin? Trends Neurosci 30, 159-166.

Craig, J.E., Han, X., Qassim, A., Hassall, M., Cooke Bailey, J.N., Kinzy, T.G., Khawaja, A.P., An, J., Marshall, H., Gharahkhani, P., Igo, R.P., Jr., Graham, S.L., Healey, P.R., Ong, J.S., Zhou, T., Siggs, O., Law, M.H., Souzeau, E., Ridge, B., Hysi, P.G., Burdon, K.P., Mills, R.A., Landers, J., Ruddle, J.B., Agar, A., Galanopoulos, A., White, A.J.R., Willoughby, C.E., Andrew, N.H., Best, S., Vincent, A.L., Goldberg, I., Radford-Smith, G., Martin, N.G., Montgomery, G.W., Vitart, V., Hoehn, R., Wojciechowski, R., Jonas, J.B., Aung, T., Pasquale, L.R., Cree, A.J., Sivaprasad, S., Vallabh, N.A., consortium, N., Eye, U.K.B., Vision, C., Viswanathan, A.C., Pasutto, F., Haines, J.L., Klaver, C.C.W., van Duijn, C.M., Casson, R.J., Foster, P.J., Khaw, P.T., Hammond, C.J., Mackey, D.A., Mitchell, P., Lotery, A.J., Wiggs, J.L., Hewitt, A.W., MacGregor, S., 2020. Multitrait analysis of glaucoma identifies new risk loci and enables polygenic prediction of disease susceptibility and progression. Nat Genet 52, 160-166.

Cringle, S.J., Yu, D.Y., Yu, P.K., Su, E.N., 2002. Intraretinal oxygen consumption in the rat in vivo. Invest Ophthalmol Vis Sci 43, 1922-1927.

Crotty, P., Sangrey, T., Levy, W.B., 2006. Metabolic energy cost of action potential velocity. J Neurophysiol 96, 1237-1246.

Cunha-Vaz, J., 1979. The blood-ocular barriers. Surv Ophthalmol 23, 279-296.

Davis, B.M., Tian, K., Pahlitzsch, M., Brenton, J., Ravindran, N., Butt, G., Malaguarnera, G., Normando, E.M., Guo, L., Cordeiro, M.F., 2017. Topical Coenzyme Q10 demonstrates mitochondrial-mediated neuroprotection in a rodent model of ocular hypertension. Mitochondrion 36, 114-123.

De Moraes, C.G., Liebmann, J.M., Levin, L.A., 2017. Detection and measurement of clinically meaningful visual field progression in clinical trials for glaucoma. Prog Retin Eye Res 56, 107-147.

De Schaepdrijver, L., Simoens, P., Lauwers, H., De Geest, J.P., 1989. Retinal vascular patterns in domestic animals. Res Vet Sci 47, 34-42.

Della Santina, L., Inman, D.M., Lupien, C.B., Horner, P.J., Wong, R.O., 2013. Differential progression of structural and functional alterations in distinct retinal ganglion cell types in a mouse model of glaucoma. Journal of Neuroscience 33, 17444-17457.

Doll, D.N., Hu, H., Sun, J., Lewis, S.E., Simpkins, J.W., Ren, X., 2015. Mitochondrial crisis in cerebrovascular endothelial cells opens the blood-brain barrier. Stroke 46, 1681-1689.

Dowling, J.E., 1987. An approachable part of the brain. Cambridge. The Retina.

Drance, S.M., Douglas, G.R., Wijsman, K., Schulzer, M., Britton, R.J., 1988. Response of blood flow to warm and cold in normal and low-tension glaucoma patients. Am J Ophthalmol 105, 35-39.

Dyer, A.H., Vahdatpour, C., Sanfeliu, A., Tropea, D., 2016. The role of Insulin-Like Growth Factor 1 (IGF-1) in brain development, maturation and neuroplasticity. Neuroscience 325, 89-99.

Ebneter, A., Chidlow, G., Wood, J.P., Casson, R.J., 2011. Protection of retinal ganglion cells and the optic nerve during short-term hyperglycemia in experimental glaucoma. Arch Ophthalmol 129, 1337-1344.

El-Danaf, R.N., Huberman, A.D., 2015. Characteristic patterns of dendritic remodeling in early-stage glaucoma: evidence from genetically identified retinal ganglion cell types. J Neurosci 35, 2329-2343.

Enroth-Cugell, C., Robson, J.G., 1966. The contrast sensitivity of retinal ganglion cells of the cat. J Physiol 187, 517-552.

Evans, D.W., Hosking, S.L., Gherghel, D., Bartlett, J.D., 2003. Contrast sensitivity improves after brimonidine therapy in primary open angle glaucoma: a case for neuroprotection. Br J Ophthalmol 87, 1463-1465.

Famiglietti, E.V., Jr., Kolb, H., 1976. Structural basis for ON-and OFF-center responses in retinal ganglion cells. Science 194, 193-195.

Ferrante, R.J., Andreassen, O.A., Jenkins, B.G., Dedeoglu, A., Kuemmerle, S., Kubilus, J.K., Kaddurah-Daouk, R., Hersch, S.M., Beal, M.F., 2000. Neuroprotective effects of creatine in a transgenic mouse model of Huntington's disease. J Neurosci 20, 4389-4397.

Flamholz, A., Phillips, R., Milo, R., 2014. The quantified cell. Mol Biol Cell 25, 3497-3500.

Flammer, J., 1994. The vascular concept of glaucoma. Surv Ophthalmol 38 Suppl, S3-6.

Flammer, J., Orgul, S., Costa, V.P., Orzalesi, N., Krieglstein, G.K., Serra, L.M., Renard, J.P., Stefansson, E., 2002. The impact of ocular blood flow in glaucoma. Prog Retin Eye Res 21, 359-393.

Funfschilling, U., Supplie, L.M., Mahad, D., Boretius, S., Saab, A.S., Edgar, J., Brinkmann, B.G., Kassmann, C.M., Tzvetanova, I.D., Mobius, W., Diaz, F., Meijer, D., Suter, U., Hamprecht, B., Sereda, M.W., Moraes, C.T., Frahm, J., Goebbels, S., Nave, K.A., 2012. Glycolytic oligodendrocytes maintain myelin and long-term axonal integrity. Nature 485, 517-521.

Gandolfi, S.A., Cimino, L., Sangermani, C., Ungaro, N., Mora, P., Tardini, M.G., 2005. Improvement of spatial contrast sensitivity threshold after surgical reduction of intraocular pressure in unilateral high-tension glaucoma. Invest Ophthalmol Vis Sci 46, 197-201.

Garway-Heath, D.F., Crabb, D.P., Bunce, C., Lascaratos, G., Amalfitano, F., Anand, N., Azuara-Blanco, A., Bourne, R.R., Broadway, D.C., Cunliffe, I.A., Diamond, J.P., Fraser, S.G., Ho, T.A., Martin, K.R., McNaught, A.I., Negi, A., Patel, K., Russell, R.A., Shah, A., Spry, P.G., Suzuki, K., White, E.T., Wormald, R.P., Xing, W., Zeyen, T.G., 2015. Latanoprost for open-angle glaucoma (UKGTS): a randomised, multicentre, placebo-controlled trial. Lancet 385, 1295-1304.

Geijssen, H.C., Greve, E.L., 1987. The spectrum of primary open angle glaucoma. I: Senile sclerotic glaucoma versus high tension glaucoma. Ophthalmic Surg 18, 207-213.

Gharahkhani, P., Burdon, K.P., Fogarty, R., Sharma, S., Hewitt, A.W., Martin, S., Law, M.H., Cremin, K., Bailey, J.N.C., Loomis, S.J., Pasquale, L.R., Haines, J.L., Hauser, M.A., Viswanathan, A.C., McGuffin, P., Topouzis, F., Foster, P.J., Graham, S.L., Casson, R.J., Chehade, M., White, A.J., Zhou, T., Souzeau, E., Landers, J., Fitzgerald, J.T., Klebe, S., Ruddle, J.B., Goldberg, I., Healey, P.R., Wellcome Trust Case Control Consortium, N.c., Mills, R.A., Wang, J.J., Montgomery, G.W., Martin, N.G., RadfordSmith, G., Whiteman, D.C., Brown, M.A., Wiggs, J.L., Mackey, D.A., Mitchell, P., MacGregor, S., Craig, J.E., 2014. Common variants near ABCA1, AFAP1 and GMDS confer risk of primary open-angle glaucoma. Nat Genet 46, 1120-1125.

Gilley, J., Coleman, M.P., 2010. Endogenous Nmnat2 is an essential survival factor for maintenance of healthy axons. PLoS Biol 8, e1000300.

Grafstein, B., Forman, D.S., 1980. Intracellular transport in neurons. Physiological Reviews 60, 1167-1283.

Graymore, C., Tansley, K., 1959. Iodoacetate poisoning of the rat retina. II. Glycolysis in the poisoned retina. Br J Ophthalmol 43, 486-493.

Haldane, J.B.S., 1929. . Origin of Life. The Rationalist Annual 148, 3-10.

Harder, J.M., Braine, C.E., Williams, P.A., Zhu, X., MacNicoll, K.H., Sousa, G.L., Buchanan, R.A., Smith, R.S., Libby, R.T., Howell, G.R., John, S.W.M., 2017. Early immune responses are independent of RGC dysfunction in glaucoma with complement component C3 being protective. Proc Natl Acad Sci U S A 114, E3839-E3848.

Harris, J.J., Attwell, D., 2012. The energetics of CNS white matter. J Neurosci 32, 356-371.

Harris, J.J., Jolivet, R., Attwell, D., 2012. Synaptic energy use and supply. Neuron 75, 762-777.

Harun-Or-Rashid, M., Pappenhagen, N., Palmer, P.G., Smith, M.A., Gevorgyan, V., Wilson, G.N., Crish, S.D., Inman, D.M., 2018. Structural and Functional Rescue of Chronic Metabolically Stressed Optic Nerves through Respiration. J Neurosci 38, 5122-5139.

Hayreh, S.S., 1996. Blood supply of the optic nerve head. Ophthalmologica 210, 285-295.

Hayreh, S.S., 2001. The blood supply of the optic nerve head and the evaluation of it - myth and reality. Prog Retin Eye Res 20, 563-593.

Heijl, A., Buchholz, P., Norrgren, G., Bengtsson, B., 2013. Rates of visual field progression in clinical glaucoma care. Acta Ophthalmol 91, 406-412.

Hendry, S.H., Reid, R.C., 2000. The koniocellular pathway in primate vision. Annu Rev Neurosci 23, 127-153.

Herculano-Houzel, S., 2009. The human brain in numbers: a linearly scaled-up primate brain. Front Hum Neurosci 3, 31.

Hitchings, R.A., Powell, D.J., Arden, G.B., Carter, R.M., 1981. Contrast sensitivity gratings in glaucoma family screening. Br J Ophthalmol 65, 515-517.

Hodgkin, A.L., Huxley, A.F., 1952. A quantitative description of membrane current and its application to conduction and excitation in nerve. J Physiol 117, 500-544.

Holland, H.D., 2006. The oxygenation of the atmosphere and oceans. Philosophical Transactions of the Royal Society B: Biological Sciences 361, 903-915.

Holman, M.C., Chidlow, G., Wood, J.P., Casson, R.J., 2010. The effect of hyperglycemia on hypoperfusion-induced injury. Invest Ophthalmol Vis Sci 51, 2197-2207.

Hosios, A.M., Hecht, V.C., Danai, L.V., Johnson, M.O., Rathmell, J.C., Steinhauser, M.L., Manalis, S.R., Vander Heiden, M.G., 2016. Amino Acids Rather than Glucose Account for the Majority of Cell Mass in Proliferating Mammalian Cells. Dev Cell 36, 540-549.

Hou, H., Moghimi, S., Proudfoot, J.A., Ghahari, E., Penteado, R.C., Bowd, C., Yang, D., Weinreb, R.N., 2020. Ganglion Cell Complex Thickness and Macular Vessel Density Loss in Primary Open-Angle Glaucoma. Ophthalmology.

Howell, G.R., Libby, R.T., Jakobs, T.C., Smith, R.S., Phalan, F.C., Barter, J.W., Barbay, J.M., Marchant, J.K., Mahesh, N., Porciatti, V., 2007. Axons of retinal ganglion cells are insulted in the optic nerve early in DBA/2J glaucoma. The Journal of cell biology 179, 1523-1537.

Howell, G.R., Soto, I., Libby, R.T., John, S.W., 2013. Intrinsic axonal degeneration pathways are critical for glaucomatous damage. Exp Neurol 246, 54-61.

Hughes, J.M., Groot, A.J., van der Groep, P., Sersansie, R., Vooijs, M., van Diest, P.J., Van Noorden, C.J., Schlingemann, R.O., Klaassen, I., 2010. Active HIF-1 in the normal human retina. J Histochem Cytochem 58, 247-254.

Hughes, W.F., 1991. Quantitation of ischemic damage in the rat retina. Exp Eye Res 53, 573-582.

Hui, F., Tang, J., Williams, P.A., McGuinness, M.B., Hadoux, X., Casson, R.J., Coote, M., Trounce, I.A., Martin, K.R., van Wijngaarden, P., G., C.J., 2020. Improvement in Inner Retinal Function in Glaucoma in Response to Nicotinamide (Vitamin B3 Supplementation: A Crossover Randomized Clinical Trial. Clinical and Experimental Ophthalmology in press.

Hui, S., Ghergurovich, J.M., Morscher, R.J., Jang, C., Teng, X., Lu, W., Esparza, L.A., Reya, T., Le, Z., Yanxiang Guo, J., White, E., Rabinowitz, J.D., 2017. Glucose feeds the TCA cycle via circulating lactate. Nature 551, 115-118.

Hwang, M., Perez, C.A., Moretti, L., Lu, B., 2008. The mTOR signaling network: insights from its role during embryonic development. Curr Med Chem 15, 1192-1208.

Ito, Y.A., Belforte, N., Cueva Vargas, J.L., Di Polo, A., 2016. A Magnetic Microbead Occlusion Model to Induce Ocular Hypertension-Dependent Glaucoma in Mice. J Vis Exp, e53731.

Ito, Y.A., Di Polo, A., 2017. Mitochondrial dynamics, transport, and quality control: A bottleneck for retinal ganglion cell viability in optic neuropathies. Mitochondrion 36, 186-192.

Jaeger, E., 1858. Ueber glaucom und seine Heilung durch Iridectomie. Druck von C. Gerold's Sohn.

Jassim, A.H., Inman, D.M., 2019. Evidence of Hypoxic Glial Cells in a Model of Ocular Hypertension. Invest Ophthalmol Vis Sci 60, 1-15.

Jewell, J.L., Guan, K.L., 2013. Nutrient signaling to mTOR and cell growth. Trends Biochem Sci 38, 233-242.

Ji, D., Li, G.Y., Osborne, N.N., 2008. Nicotinamide attenuates retinal ischemia and light insults to neurones. Neurochem Int 52, 786-798.

Jonas, J.B., Muller-Bergh, J.A., Schlotzer-Schrehardt, U.M., Naumann, G.O., 1990. Histomorphometry of the human optic nerve. Invest Ophthalmol Vis Sci 31, 736-744.

Junge, W., Nelson, N., 2015. ATP synthase. Annu Rev Biochem 84, 631-657.

Khawaja, A.P., Crabb, D.P., Jansonius, N.M., 2013. The role of ocular perfusion pressure in glaucoma cannot be studied with multivariable regression analysis applied to surrogates. Invest Ophthalmol Vis Sci 54, 4619-4620.

Kim, J.W., Tchernyshyov, I., Semenza, G.L., Dang, C.V., 2006. HIF-1-mediated expression of pyruvate dehydrogenase kinase: a metabolic switch required for cellular adaptation to hypoxia. Cell Metab 3, 177-185.

Kirwan, J.F., Hustler, A., Bobat, H., Toms, L., Crabb, D.P., McNaught, A.I., 2014. Portsmouth visual field database: an audit of glaucoma progression. Eye (Lond) 28, 974-979.

Klivenyi, P., Ferrante, R.J., Matthews, R.T., Bogdanov, M.B., Klein, A.M., Andreassen, O.A., Mueller, G., Wermer, M., Kaddurah-Daouk, R., Beal, M.F., 1999. Neuroprotective effects of creatine in a transgenic animal model of amyotrophic lateral sclerosis. Nat Med 5, 347-350.

Kniesel, U., Wolburg, H., 2000. Tight junctions of the blood-brain barrier. Cell Mol Neurobiol 20, 57-76.

Kolb, H., 1970. Organization of the outer plexiform layer of the primate retina: electron microscopy of Golgi-impregnated cells. Philos Trans R Soc Lond B Biol Sci 258, 261-283.

Kolb, H., Famiglietti, E.V., 1974. Rod and cone pathways in the inner plexiform layer of cat retina. Science 186, 47-49.

Kong, Y.X., Crowston, J.G., Vingrys, A.J., Trounce, I.A., Bui, V.B., 2009. Functional changes in the retina during and after acute intraocular pressure elevation in mice. Invest Ophthalmol Vis Sci 50, 5732-5740.

Laughlin, S.B., de Ruyter van Steveninck, R.R., Anderson, J.C., 1998. The metabolic cost of neural information. Nat Neurosci 1, 36-41.

Lazcano, A., Miller, S.L., 1999. On the origin of metabolic pathways. J Mol Evol 49, 424-431.

Lee, D., Shim, M.S., Kim, K.Y., Noh, Y.H., Kim, H., Kim, S.Y., Weinreb, R.N., Ju, W.K., 2014a. Coenzyme Q10 inhibits glutamate excitotoxicity and oxidative stress-mediated mitochondrial alteration in a mouse model of glaucoma. Invest Ophthalmol Vis Sci 55, 993-1005.

Lee, J.M., Caprioli, J., Nouri-Mahdavi, K., Afifi, A.A., Morales, E., Ramanathan, M., Yu, F., Coleman, A.L., 2014b. Baseline prognostic factors predict rapid visual field deterioration in glaucoma. Invest Ophthalmol Vis Sci 55, 2228-2236.

Lee, S., Van Bergen, N.J., Kong, G.Y., Chrysostomou, V., Waugh, H.S., O'Neill, E.C., Crowston, J.G., Trounce, I.A., 2011. Mitochondrial dysfunction in glaucoma and emerging bioenergetic therapies. Exp Eye Res 93, 204-212.

Lee, Y., Morrison, B.M., Li, Y., Lengacher, S., Farah, M.H., Hoffman, P.N., Liu, Y., Tsingalia, A., Jin, L., Zhang, P.W., Pellerin, L., Magistretti, P.J., Rothstein, J.D., 2012. Oligodendroglia metabolically support axons and contribute to neurodegeneration. Nature 487, 443-448.

Leske, M.C., 2009. Ocular perfusion pressure and glaucoma: clinical trial and epidemiologic findings. Curr Opin Ophthalmol 20, 73-78.

Leske, M.C., Wu, S.-Y., Hennis, A., Honkanen, R., Nemesure, B., Group, B.S., 2008. Risk factors for incident open-angle glaucoma: the Barbados Eye Studies. Ophthalmology 115, 85-93.

Levkovitch-Verbin, H., Quigley, H.A., Martin, K.R., Valenta, D., Baumrind, L.A., Pease, M.E., 2002. Translimbal laser photocoagulation to the trabecular meshwork as a model of glaucoma in rats. Invest Ophthalmol Vis Sci 43, 402-410.

Lindsay, K.J., Du, J., Sloat, S.R., Contreras, L., Linton, J.D., Turner, S.J., Sadilek, M., Satrustegui, J., Hurley, J.B., 2014. Pyruvate kinase and aspartate-glutamate carrier distributions reveal key metabolic links between neurons and glia in retina. Proc Natl Acad Sci U S A 111, 15579-15584.

Lippman, F., 1941. Metabolic generation and utilization of phosphate bond energy. Advances in Enzymololgy 1, 99-162.

Locasale, J.W., Cantley, L.C., 2011. Metabolic flux and the regulation of mammalian cell growth. Cell Metab 14, 443-451.

Lowry, O.H., Roberts, N.R., Schulz, D.W., Clow, J.E., Clark, J.R., 1961. Quantitative histochemistry of retina. II. Enzymes of glucose metabolism. J Biol Chem 236, 2813-2820.

MacGregor, S., Ong, J.S., An, J., Han, X., Zhou, T., Siggs, O.M., Law, M.H., Souzeau, E., Sharma, S., Lynn, D.J., Beesley, J., Sheldrick, B., Mills, R.A., Landers, J., Ruddle, J.B., Graham, S.L., Healey, P.R., White, A.J.R., Casson, R.J., Best, S., Grigg, J.R., Goldberg, I., Powell, J.E., Whiteman, D.C., Radford-Smith, G.L., Martin, N.G., Montgomery, G.W., Burdon, K.P., Mackey, D.A., Gharahkhani, P., Craig, J.E., Hewitt, A.W., 2018. Genome-wide association study of intraocular pressure uncovers new pathways to glaucoma. Nat Genet 50, 1067-1071.

Mack, T.G., Reiner, M., Beirowski, B., Mi, W., Emanuelli, M., Wagner, D., Thomson, D., Gillingwater, T., Court, F., Conforti, L., Fernando, F.S., Tarlton, A., Andressen, C., Addicks, K., Magni, G., Ribchester, R.R., Perry, V.H., Coleman, M.P., 2001. Wallerian degeneration of injured axons and synapses is delayed by a Ube4b/Nmnat chimeric gene. Nat Neurosci 4, 1199-1206.

Matthews, R.T., Yang, L., Browne, S., Baik, M., Beal, M.F., 1998. Coenzyme Q10 administration increases brain mitochondrial concentrations and exerts neuroprotective effects. Proc Natl Acad Sci U S A 95, 8892-8897.

McCulloch, W.S., Pitts, W., 1943. A logical calculus of the ideas immanent in nervous activity. The bulletin of mathematical biophysics 5, 115-133.

Melena, J., Safa, R., Graham, M., Casson, R.J., Osborne, N.N., 2003. The monocarboxylate transport inhibitor, alpha-cyano-4-hydroxycinnamate, has no effect on retinal ischemia. Brain Res 989, 128-134.

Memarzadeh, F., Ying-Lai, M., Chung, J., Azen, S.P., Varma, R., 2010. Blood pressure, perfusion pressure, and open-angle glaucoma: the Los Angeles Latino Eye Study. Investigative ophthalmology & visual science 51, 2872-2877.

Millecamps, S., Julien, J.P., 2013. Axonal transport deficits and neurodegenerative diseases. Nat Rev Neurosci 14, 161-176.

Minckler, D.S., McLean, I.W., Tso, M.O., 1976. Distribution of axonal and glial elements in the rhesus optic nerve head studied by electron microscopy. Am J Ophthalmol 82, 179-187.

Mironova, Y.A., Giger, R.J., 2013. Where no synapses go: gatekeepers of circuit remodeling and synaptic strength. Trends Neurosci 36, 363-373.

Mitchell, P., 1966. Chemiosmotic coupling in oxidative and photosynthetic phosphorylation. Biol Rev Camb Philos Soc 41, 445-502.

Morgan, J.E., Jeffery, G., Foss, A.J., 1998. Axon deviation in the human lamina cribrosa. Br J Ophthalmol 82, 680-683.

Morquette, B., Morquette, P., Agostinone, J., Feinstein, E., McKinney, R.A., Kolta, A., Di Polo, A., 2015. REDD2-mediated inhibition of mTOR promotes dendrite retraction induced by axonal injury. Cell Death Differ 22, 612-625.

Nair, A.B., Jacob, S., 2016. A simple practice guide for dose conversion between animals and human. J Basic Clin Pharm 7, 27-31.

Nicolela, M.T., Drance, S.M., 1996. Various glaucomatous optic nerve appearances: clinical correlations. Ophthalmology 103, 640-649.

Noell, W.K., 1951. Site of asphyxial block in mammalian retinae. J Appl Physiol 3, 489-500.

Nucci, C., Tartaglione, R., Cerulli, A., Mancino, R., Spano, A., Cavaliere, F., Rombola, L., Bagetta, G., Corasaniti, M.T., Morrone, L.A., 2007. Retinal damage caused by high intraocular pressure-induced transient ischemia is prevented by coenzyme Q10 in rat. Int Rev Neurobiol 82, 397-406.

Okawa, H., Sampath, A.P., Laughlin, S.B., Fain, G.L., 2008. ATP consumption by mammalian rod photoreceptors in darkness and in light. Curr Biol 18, 1917-1921.

Oldendorf, W.H., Cornford, M.E., Brown, W.J., 1977. The large apparent work capability of the blood-brain barrier: a study of the mitochondrial content of capillary endothelial cells in brain and other tissues of the rat. Ann Neurol 1, 409-417.

Onda, E., Cioffi, G.A., Bacon, D.R., Van Buskirk, E.M., 1995. Microvasculature of the human optic nerve. Am J Ophthalmol 120, 92-102.

Pang, J.J., Frankfort, B.J., Gross, R.L., Wu, S.M., 2015. Elevated intraocular pressure decreases response sensitivity of inner retinal neurons in experimental glaucoma mice. Proc Natl Acad Sci U S A 112, 2593-2598.

Park, K.K., Liu, K., Hu, Y., Smith, P.D., Wang, C., Cai, B., Xu, B., Connolly, L., Kramvis, I., Sahin, M., He, Z., 2008. Promoting axon regeneration in the adult CNS by modulation of the PTEN/mTOR pathway. Science 322, 963-966.

Parrish, R., Gass, J.D., Anderson, D.R., 1982. Outer retina ischemic infarction--a newly recognized complication of cataract extraction and closed vitrectomy. Part 2. An animal model. Ophthalmology 89, 1472-1477.

Pasteur, L., 1861. Influence de l'oxygene sur le developpement de la levure et la fermentation alcoolique. Annales de Chimie et de Physique.

Pellerin, L., Magistretti, P.J., 1994. Glutamate uptake into astrocytes stimulates aerobic glycolysis: a mechanism coupling neuronal activity to glucose utilization. Proc Natl Acad Sci U S A 91, 10625-10629.

Perge, J.A., Koch, K., Miller, R., Sterling, P., Balasubramanian, V., 2009. How the optic nerve allocates space, energy capacity, and information. J Neurosci 29, 7917-7928.

Petit, L., Ma, S., Cipi, J., Cheng, S.Y., Zieger, M., Hay, N., Punzo, C., 2018. Aerobic Glycolysis Is Essential for Normal Rod Function and Controls Secondary Cone Death in Retinitis Pigmentosa. Cell Rep 23, 2629-2642.

Poitry-Yamate, C.L., Poitry, S., Tsacopoulos, M., 1995. Lactate released by Muller glial cells is metabolized by photoreceptors from mammalian retina. J Neurosci 15, 5179-5191.

Prass, K., Royl, G., Lindauer, U., Freyer, D., Megow, D., Dirnagl, U., Stockler-Ipsiroglu, G., Wallimann, T., Priller, J., 2007. Improved reperfusion and neuroprotection by creatine in a mouse model of stroke. J Cereb Blood Flow Metab 27, 452-459.

Quigley, H.A., Addicks, E.M., Green, W.R., Maumenee, A., 1981. Optic nerve damage in human glaucoma: II. The site of injury and susceptibility to damage. Archives of ophthalmology 99, 635-649.

Quigley, H.A., Anderson, D.R., 1977. Distribution of axonal transport blockade by acute intraocular pressure elevation in the primate optic nerve head. Investigative ophthalmology & visual science 16, 640-644.

Quigley, H.A., Guy, J., Anderson, D.R., 1979. Blockade of rapid axonal transport. Effect of intraocular pressure elevation in primate optic nerve. Arch Ophthalmol 97, 525-531.

Radius, R.L., Anderson, D.R., 1981. Rapid axonal transport in primate optic nerve. Distribution of pressure-induced interruption. Arch Ophthalmol 99, 650-654.

Raj, A., Chen, Y.H., 2011. The wiring economy principle: connectivity determines anatomy in the human brain. PLoS One 6, e14832.

Rangaraju, V., Calloway, N., Ryan, T.A., 2014. Activity-driven local ATP synthesis is required for synaptic function. Cell 156, 825-835.

Reichenbach, A., Wurm, A., Pannicke, T., Iandiev, I., Wiedemann, P., Bringmann, A., 2007. Muller cells as players in retinal degeneration and edema. Graefes Arch Clin Exp Ophthalmol 245, 627-636.

Risner, M.L., Pasini, S., Cooper, M.L., Lambert, W.S., Calkins, D.J., 2018. Axogenic mechanism enhances retinal ganglion cell excitability during early progression in glaucoma. Proc Natl Acad Sci U S A 115, E2393-E2402.

Rogatzki, M.J., Ferguson, B.S., Goodwin, M.L., Gladden, L.B., 2015. Lactate is always the end product of glycolysis. Front Neurosci 9, 22.

Sagan, L., 1967. On the origin of mitosing cells. J Theor Biol 14, 255-274.

Sajic, M., Mastrolia, V., Lee, C.Y., Trigo, D., Sadeghian, M., Mosley, A.J., Gregson, N.A., Duchen, M.R., Smith, K.J., 2013. Impulse conduction increases mitochondrial transport in adult mammalian peripheral nerves in vivo. PLoS Biol 11, e1001754.

Schober, M.S., Chidlow, G., Wood, J.P., Casson, R.J., 2008. Bioenergetic-based neuroprotection and glaucoma. Clin Exp Ophthalmol 36, 377-385.

Schrodinger, E., 1944. What is life? The Physical Aspect of the Living Cell. Cambridge University Press.

Seagroves, T.N., Ryan, H.E., Lu, H., Wouters, B.G., Knapp, M., Thibault, P., Laderoute, K., Johnson, R.S., 2001. Transcription factor HIF-1 is a necessary mediator of the pasteur effect in mammalian cells. Mol Cell Biol 21, 3436-3444.

Sia, P.I., Wood, J.P.M., Chidlow, G., Casson, R., 2019. Creatine is Neuroprotective to Retinal Neurons In Vitro But Not In Vivo. Invest Ophthalmol Vis Sci 60, 4360-4377.

Sieving, P.A., Frishman, L.J., Steinberg, R.H., 1986. Scotopic threshold response of proximal retina in cat. J Neurophysiol 56, 1049-1061.

Singh, L.N., Crowston, J.G., Lopez Sanchez, M.I.G., Van Bergen, N.J., Kearns, L.S., Hewitt, A.W., Yazar, S., Mackey, D.A., Wallace, D.C., Trounce, I.A., 2018. Mitochondrial DNA Variation and Disease Susceptibility in Primary Open-Angle Glaucoma. Invest Ophthalmol Vis Sci 59, 4598-4602.

Smith, G.G., Baird, C.D., 1952. Survival time of retinal cells when deprived of their blood supply by increased intraocular pressure. Am J Ophthalmol 35, 133-136.

Sradhanjali, S., Tripathy, D., Rath, S., Mittal, R., Reddy, M.M., 2017. Overexpression of pyruvate dehydrogenase kinase 1 in retinoblastoma: A potential therapeutic opportunity for targeting vitreous seeds and hypoxic regions. PLoS One 12, e0177744.

Sullivan, P.G., Geiger, J.D., Mattson, M.P., Scheff, S.W., 2000. Dietary supplement creatine protects against traumatic brain injury. Ann Neurol 48, 723-729.

Takihara, Y., Inatani, M., Eto, K., Inoue, T., Kreymerman, A., Miyake, S., Ueno, S., Nagaya, M., Nakanishi, A., Iwao, K., Takamura, Y., Sakamoto, H., Satoh, K., Kondo, M., Sakamoto, T., Goldberg, J.L., Nabekura, J., Tanihara, H., 2015. In vivo imaging of axonal transport of mitochondria in the diseased and aged mammalian CNS. Proc Natl Acad Sci U S A 112, 10515-10520.

Tan, P.E., Yu, P.K., Balaratnasingam, C., Cringle, S.J., Morgan, W.H., McAllister, I.L., Yu, D.Y., 2012. Quantitative confocal imaging of the retinal microvasculature in the human retina. Invest Ophthalmol Vis Sci 53, 5728-5736.

Tezel, G., 2006. Oxidative stress in glaucomatous neurodegeneration: mechanisms and consequences. Prog Retin Eye Res 25, 490-513.

Tielsch, J.M., Katz, J., Sommer, A., Quigley, H.A., Javitt, J.C., 1995. Hypertension, perfusion pressure, and primary open-angle glaucoma: a population-based assessment. Archives of ophthalmology 113, 216-221.

Tirard, S., 2017. J. B. S. Haldane and the origin of life. J Genet 96, 735-739.

Toh, T., Ruddle, J.B., Coote, M.A., Crowston, J.G., 2011. Preservation of myelinated nerve fibres in advanced glaucoma. Clin Exp Ophthalmol 39, 473-478.

Tout, S., Chan-Ling, T., Hollander, H., Stone, J., 1993. The role of Muller cells in the formation of the blood-retinal barrier. Neuroscience 55, 291-301.

Trevisiol, A., Saab, A.S., Winkler, U., Marx, G., Imamura, H., Mobius, W., Kusch, K., Nave, K.A., Hirrlinger, J., 2017. Monitoring ATP dynamics in electrically active white matter tracts. Elife 6.

Tribble, J.R., Vasalauskaite, A., Redmond, T., Young, R.D., Hassan, S., Fautsch, M.P., Sengpiel, F., Williams, P.A., Morgan, J.E., 2019. Midget retinal ganglion cell dendritic and mitochondrial degeneration is an early feature of human glaucoma. Brain Commun 1, fcz035.

Tsacopoulos, M., Coles, J.A., Van de Werve, G., 1987. The supply of metabolic substrate from glia to photoreceptors in the retina of the honeybee drone. J Physiol (Paris) 82, 279-287.

Tsacopoulos, M., Veuthey, A.L., Saravelos, S.G., Perrottet, P., Tsoupras, G., 1994. Glial cells transform glucose to alanine, which fuels the neurons in the honeybee retina. J Neurosci 14, 1339-1351.

Turrens, J.F., 2003. Mitochondrial formation of reactive oxygen species. J Physiol 552, 335-344.

Urbanska, M., Gozdz, A., Swiech, L.J., Jaworski, J., 2012. Mammalian target of rapamycin complex 1 (mTORC1) and 2 (mTORC2) control the dendritic arbor morphology of hippocampal neurons. J Biol Chem 287, 30240-30256.

Van Bergen, N.J., Crowston, J.G., Craig, J.E., Burdon, K.P., Kearns, L.S., Sharma, S., Hewitt, A.W., Mackey, D.A., Trounce, I.A., 2015. Measurement of systemic mitochondrial function in advanced primary open-angle glaucoma and leber hereditary optic neuropathy. PloS one 10.

Van Bergen, N.J., Crowston, J.G., Kearns, L.S., Staffieri, S.E., Hewitt, A.W., Cohn, A.C., Mackey, D.A., Trounce, I.A., 2011. Mitochondrial oxidative phosphorylation compensation may preserve vision in patients with OPA1-linked autosomal dominant optic atrophy. PLoS One 6, e21347.

Vander Heiden, M.G., Cantley, L.C., Thompson, C.B., 2009. Understanding the Warburg effect: the metabolic requirements of cell proliferation. Science 324, 1029-1033.

Ventura, L.M., Porciatti, V., 2006. Pattern electroretinogram in glaucoma. Curr Opin Ophthalmol 17, 196-202.

Vrabec, F., 1976. Glaucomatous cupping of the human optic disk: a neuro-histologic study. Albrecht Von Graefes Arch Klin Exp Ophthalmol 198, 223-234.

Wang, J., Zhai, Q., Chen, Y., Lin, E., Gu, W., McBurney, M.W., He, Z., 2005. A local mechanism mediates NAD-dependent protection of axon degeneration. J Cell Biol 170, 349-355.

Wang, L., Dong, J., Cull, G., Fortune, B., Cioffi, G.A., 2003. Varicosities of intraretinal ganglion cell axons in human and nonhuman primates. Invest Ophthalmol Vis Sci 44, 2-9.

Wang, L., Tornquist, P., Bill, A., 1997a. Glucose metabolism in pig outer retina in light and darkness. Acta Physiol Scand 160, 75-81.

Wang, L., Tornquist, P., Bill, A., 1997b. Glucose metabolism of the inner retina in pigs in darkness and light. Acta Physiol Scand 160, 71-74.

Warburg, O., 1930. in: Otto Warburg, T.f.t.G.b.F.D. (Ed.), The Metabolism of Tumors: Investigations from the Kaiser Wilhelm Institute for Biology, Berlin-Dahlem. London, Constable & Co. Ltd, London.

Weiss, H., 1972. The carbohydrate reserve in the vitreous body and retina of the rabbit's eye during and after pressure ischemia and insulin hypoglycaemia. Ophthalmic Research 3, 360-371.

Weiss, M.C., Sousa, F.L., Mrnjavac, N., Neukirchen, S., Roettger, M., Nelson-Sathi, S., Martin, W.F., 2016. The physiology and habitat of the last universal common ancestor. Nat Microbiol 1, 16116.

Werner, A.C., Shen, L.Q., 2019. A Review of OCT Angiography in Glaucoma. Semin Ophthalmol 34, 279-286.

Whitmore, A.V., Libby, R.T., John, S.W., 2005. Glaucoma: thinking in new ways-a role for autonomous axonal self-destruction and other compartmentalised processes? Prog Retin Eye Res 24, 639-662.

Williams, P.A., Harder, J.M., Cardozo, B.H., Foxworth, N.E., John, S.W.M., 2018. Nicotinamide treatment robustly protects from inherited mouse glaucoma. Commun Integr Biol 11, e1356956.

Williams, P.A., Harder, J.M., Foxworth, N.E., Cardozo, B.H., Cochran, K.E., John, S.W.M., 2017a. Nicotinamide and WLD(S) Act Together to Prevent Neurodegeneration in Glaucoma. Front Neurosci 11, 232.

Williams, P.A., Harder, J.M., Foxworth, N.E., Cochran, K.E., Philip, V.M., Porciatti, V., Smithies, O., John, S.W., 2017b. Vitamin B3 modulates mitochondrial vulnerability and prevents glaucoma in aged mice. Science 355, 756-760.

Williams, P.A., Harder, J.M., Guymer, C., Wood, J.P., Daskalakis, E., Chidlow, G., Cardozo, B.H., Foxworth, N.E., Cochran, K.E., Ouellette, T.B., Wheelock, C.E., Casson, R.J., John, S.W., 2020. Oral pyruvate prevents glaucomatous neurodegeneration. bioRxiv, 2020.2005.2002.072215.

Williams, P.A., Harder, J.M., John, S.W.M., 2017c. Glaucoma as a Metabolic Optic Neuropathy: Making the Case for Nicotinamide Treatment in Glaucoma. J Glaucoma 26, 1161-1168.

Williams, P.A., Morgan, J.E., Votruba, M., 2010. Opa1 deficiency in a mouse model of dominant optic atrophy leads to retinal ganglion cell dendropathy. Brain 133, 2942-2951.

Williams, P.A., Piechota, M., von Ruhland, C., Taylor, E., Morgan, J.E., Votruba, M., 2012. Opa1 is essential for retinal ganglion cell synaptic architecture and connectivity. Brain 135, 493-505.

Williams, T.A., Foster, P.G., Cox, C.J., Embley, T.M., 2013. An archaeal origin of eukaryotes supports only two primary domains of life. Nature 504, 231-236.

Winkler, B.S., 1981a. Glycolytic and oxidative metabolism in relation to retinal function. J Gen Physiol 77, 667-692.

Winkler, B.S., 1981b. Glycolytic and oxidative metabolism in relation to retinal function. J Gen Physiol 77, 667-692.

Winkler, B.S., Pourcho, R.G., Starnes, C., Slocum, J., Slocum, N., 2003. Metabolic mapping in mammalian retina: a biochemical and 3H-2-deoxyglucose autoradiographic study. Exp Eye Res 77, 327-337.

Wood, J.P., Chidlow, G., Graham, M., Osborne, N.N., 2005. Energy substrate requirements for survival of rat retinal cells in culture: the importance of glucose and monocarboxylates. J Neurochem 93, 686-697.

Xu, C.J., Klunk, W.E., Kanfer, J.N., Xiong, Q., Miller, G., Pettegrew, J.W., 1996. Phosphocreatine-dependent glutamate uptake by synaptic vesicles. A comparison with atp-dependent glutamate uptake. J Biol Chem 271, 13435-13440.

Yanoff, M., Duker, J.S., Augsburger, J.J., 2009. Ophthalmology. Mosby Elsevier.

Yokota, S., Takihara, Y., Arimura, S., Miyake, S., Takamura, Y., Yoshimura, N., Inatani, M., 2015. Altered Transport Velocity of Axonal Mitochondria in Retinal Ganglion Cells After Laser-Induced Axonal Injury In Vitro. Invest Ophthalmol Vis Sci 56, 8019-8025.

Yu, D.Y., Cringle, S.J., 2001. Oxygen distribution and consumption within the retina in vascularised and avascular retinas and in animal models of retinal disease. Prog Retin Eye Res 20, 175-208.

Yu, D.Y., Cringle, S.J., Balaratnasingam, C., Morgan, W.H., Yu, P.K., Su, E.N., 2013. Retinal ganglion cells: Energetics, compartmentation, axonal transport, cytoskeletons and vulnerability. Prog Retin Eye Res 36, 217-246.

Yu, P.K., McAllister, I.L., Morgan, W.H., Cringle, S.J., Yu, D.Y., 2017. Inter-Relationship of Arterial Supply to Human Retina, Choroid, and Optic Nerve Head Using Micro Perfusion and Labeling. Invest Ophthalmol Vis Sci 58, 3565-3574.

Zhu, S., Li, M., Figueroa, B.E., Liu, A., Stavrovskaya, I.G., Pasinelli, P., Beal, M.F., Brown, R.H., Jr., Kristal, B.S., Ferrante, R.J., Friedlander, R.M., 2004. Prophylactic creatine administration mediates neuroprotection in cerebral ischemia in mice. J Neurosci 24, 5909-5912.

Zhu, X.H., Qiao, H., Du, F., Xiong, Q., Liu, X., Zhang, X., Ugurbil, K., Chen, W., 2012. Quantitative imaging of energy expenditure in human brain. Neuroimage 60, 2107-2117.